Published in Computers & Fluids 102 (2014) 131-147
http://dx.doi.org/10.1016/j.compfluid.2014.06.020

# Very Efficient High-Order Hyperbolic Schemes for Time-Dependent Advection-Diffusion Problems: Third-, Fourth-, and Sixth-Order

Alireza Mazaheri*

*NASA Langley Research Center, Hampton, Virginia 23681, USA.*

Hiroaki Nishikawa

*National Institute of Aerospace, Hampton, Virginia 23666, USA.*

**Abstract**

In this paper, we construct very efficient high-order schemes for general time-dependent advection-diffusion problems, based on the first-order hyperbolic system method. Extending the previous work on the second-order time-dependent hyperbolic advection-diffusion scheme [Mazaheri and Nishikawa, NASA/TM-2014-218175, 2014], we construct third-, fourth-, and sixth-order accurate schemes by modifying the source term discretization. In this paper, two techniques for the source term discretization are proposed; 1) reformulation of the source terms with their divergence forms, and 2) correction to the trapezoidal rule for the source term discretization. We construct spatially third- and fourth-order schemes from the former technique. These schemes require computations of the gradients and second-derivatives of the source terms. From the latter technique, we construct spatially third-, fourth-, and sixth-order schemes by using the gradients and second-derivatives for the source terms, except the fourth-order scheme, which does not require the second derivatives of the source term and thus is even less computationally expensive than the third-order schemes. We then construct high-order time-accurate schemes by incorporating a high-order backward difference formula as a source term. These schemes are very efficient in that high-order accuracy is achieved for both the solution and the gradient only by the improved source term discretization. A very rapid Newton-type convergence is achieved by a compact second-order Jacobian formulation. The numerical results are presented for both steady and time-dependent linear and nonlinear advection-diffusion problems, demonstrating these powerful features.

*Corresponding author
*Email address:* ali.r.mazaheri@nasa.gov (Alireza Mazaheri )

*Keywords:* Higher-Order, Residual Distribution, Unsteady, Nonlinear, Navier-Stokes

## 1. Introduction

In this paper, we construct very efficient high-order schemes for general time-dependent advection-diffusion problems, based on the first-order hyperbolic system method [1, 2]. In this method, the diffusion term is reformulated as a hyperbolic system, leading to the unification of advection and diffusion as a single hyperbolic system [2]. The drastic change in the type of equations, parabolic to hyperbolic, brings several dramatic improvements in the construction of numerical schemes: hyperbolic schemes for diffusion, the same order of accuracy for the solution and the gradients, orders-of-magnitude convergence acceleration, etc., which have been demonstrated for steady diffusion and viscous problems in Refs. [1, 2, 3, 4, 5] and unsteady advection-diffusion problems in Ref. [6]. It is based on the reformulation of the governing equations, and therefore applicable to any discretization method. In this work, we consider a Residual-Distribution (RD) method [7], which has been well developed for hyperbolic systems and has a superior feature of achieving second-order accuracy in a compact stencil.

In the previous work [6], we extended the hyperbolic method, for the first time, to time-accurate computations by an implicit time-integration method based on the second-order backward difference formula. The resulting scheme was applied to various time-dependent problems, demonstrating second-order accuracy for the solution and the gradient achieved at all interior and boundary nodes in uniform and nonuniform grids at every physical time step, and rapid convergence for solving implicit-residual equations by Newton's method (i.e., less than 5 iterations per physical time step), which is possible by the compactness of the RD schemes. As a consequence of the first-order re-formulation of the equation, the number of linear relaxations performed at every Newton iteration was shown to increase only linearly with the grid size, not quadratically as typical for diffusion problems. The efficiency of the developed second-order schemes was demonstrated for linear and nonlinear advection-diffusion problems on highly refined grids, up to 30000 nodes.

In this paper, we propose a very simple extension of the second-order schemes to higher-order. We show that high-order spatial accuracy can be achieved simply by modifying the source term discretization. There are two approaches to the source term discretization: 1) reformulation of the source terms with their divergence forms, and 2) correction to the

trapezoidal rule for the source term discretization. The former technique is based on the divergence formulation of source terms proposed in Ref. [8]: write the source term in the divergence form and discretize it in the same way as the flux divergence term. The latter is based on a high-order correction to the trapezoidal rule, and thus called here the generalized trapezoidal rule. In either case, high-order accuracy is achieved by making low-order truncation error terms proportional to the residual, which thus vanish in the steady state and yield high-order accuracy. We solve the resulting implicit-residual equations by an implicit solver based on the second-order Jacobian matrix developed in the previous work [6]. As we will show, the implicit solver is as powerful as Newton's method; e.g., eight orders of magnitude reduction can be achieved in 10 iterations. To enable time-accurate computations, we employ high-order versions of the backward difference formulas (BDF), which are incorporated as source terms, and solve the implicit-residual equations by the implicit solver over each physical time step. In this manner, the steady state is made equivalent to the next physical time with all the benefits of the hyperbolic method retained. We note that the choice of the implicit time stepping method is independent of the developed high-order RD schemes, and thus other methods such as implicit Runge-Kutta methods or space-time methods can also be employed.

The high-order RD schemes developed in this work are significantly different from other high-order RD schemes in that our schemes are based on the first-order hyperbolic system formulation of the advection-diffusion equation [2]. In this approach, the loss of high-order accuracy in the intermediate Reynolds number, as discussed in Refs. [9, 10, 11], cannot occur because the advective and diffusive terms are fully integrated into a single hyperbolic system. If the original advection-diffusion equation is discretized, a high-order RD scheme needs to be developed for the diffusion term (i.e., second derivative) and then carefully combined with an advection scheme, e.g. by using a blending parameter as described in Ref. [10], to avoid the loss of accuracy. Furthermore, while high-order RD schemes based on high-order elements require extra degrees of freedom for each variable, our schemes are based on linear elements for any order of accuracy but require extra gradient variable to be added to the solution vector. Note that the number of extra variables in the high-order elements increase for higher-order accuracy, but the number of extra variables required in our approach is fixed and independent of the order of accuracy. Our approach is somewhat similar to those in Refs. [12, 13, 14], but again is significantly different by the use of first-order hyperbolic

system formulation of the advection-diffusion equation and by the source term discretization techniques. It is emphasized that our schemes require only the first and second derivatives of the source term, or in some cases the first derivatives only; they do not require the gradient computation for the solution variables.

The third-order schemes developed in this paper are similar to the third-order finite-volume scheme of Katz and Sankaran [15, 16] in that the second-order truncation error is eliminated by making it proportional to the residual and the upgrade is achieved by second-order accurate gradients. However, as we demonstrate in this paper, the proposed high-order RD schemes have several superior features: 1) implicit solver can be constructed by the Jacobian derived from a compact second-order RD scheme, 2) gradient computations are required for the source terms only, and not for the solution, 3) stiffness due to the second derivative of the diffusion term is completely eliminated, 4) higher-order schemes can be constructed beyond third-order (in extending it to multi-dimensions), 5) the same order of accuracy is achieved for the gradients, as well. In particular, the fourth-order scheme constructed in Section 5 is remarkably more efficient because it does not require second derivatives of the source term, which are required in the schemes described in Refs. [15, 16].

In this paper, we focus on one-dimensional linear and nonlinear advection-diffusion problems. It certainly serves as a basis for the development of high-order multi-dimensional RD schemes for more complex equations. Yet, more importantly, the one-dimensional high-order schemes developed in this paper could potentially bring significant improvements to practical problems such as material thermal response calculations of thermal protection systems of atmospheric entry vehicles [17, 18, 19], and the experimental aeroheating data reduction [20, 21], which are based on one-dimensional analyses and routinely used in industries (e.g. NASA). The extension to higher dimensions is beyond the scope of the paper; it will be addressed in a subsequent paper.

The paper is organized as follows. In the next section, the time-dependent hyperbolic advection-diffusion system is described. In Section 3, a compact second-order residual-distribution scheme, a steady solver, and the second-order discretization are discussed. In Section 4, the third- and fourth-order RD schemes with source term reformulation are proposed. In Section 5, the third-, fourth, and sixth-order RD schemes with source term discretization are developed and proposed. Numerical results are then presented in Section 6. Finally, Section 7 concludes the study with remarks.

## 2. Time-dependent Hyperbolic Advection-Diffusion System

We start with a linear advection-diffusion equation to simplify the discussion. We will extend the discussion later to a more general nonlinear advection-diffusion equation.

Consider the one-dimensional (1-D) time-dependent advection-diffusion equation:

$$\partial_t u + a\,\partial_x u = \nu\,\partial_{xx} u + \tilde{S}(x), \tag{1}$$

where $a$ and $\nu$ are both taken to be positive constant, and $\tilde{S}$ is the source term. We will follow the procedure we described in Ref. [6] and rewrite the above equation as a first-order hyperbolic advection-diffusion system:

$$\partial_\tau u = -a\,\partial_x u + \nu\,\partial_x p - \frac{\alpha}{\Delta t} u + S(x), \tag{2}$$

$$\partial_\tau p = (\partial_x u - p)/T_r, \tag{3}$$

where the relaxation time, $T_r > 0$, is arbitrary and defined as described in Ref. [6], and $S$ includes any existing source terms from the advection-diffusion problem, $\tilde{S}$, as well as any additional terms that arise from the implicit time-stepping scheme, $\Delta t$ is the physical time steps, and $\tau$ is the pseudo time step. Note that the $\partial_t p$ is taken as pseudo time derivative, $\partial_\tau p$.

The variable $\alpha$ depends on the order of the Backward-Differencing-Formula (BDF): 1 for the 1st-order (BDF1), 3/2 for the second-order (BDF2), 11/6 for the third-order (BDF3), 25/12 for the fourth-order, and 147/60 for the sixth-order time discretizations (see Table 1). The remaining terms in the BDF are stored in the source term function $S(x)$. It is well

Table 1: BDF coefficients.

| BDF Order | $u^{n+1}$ | $u^n$ | $u^{n+1}$ | $u^{n+2}$ | $u^{n+3}$ | $u^{n+4}$ | $u^{n+5}$ |
|---|---|---|---|---|---|---|---|
| 1 | 1 | -1 | | | | | |
| 2 | $\frac{3}{2}$ | -2 | $\frac{1}{2}$ | | | | |
| 3 | $\frac{11}{6}$ | -3 | $\frac{3}{2}$ | $-\frac{1}{3}$ | | | |
| 4 | $\frac{25}{12}$ | -4 | 3 | $-\frac{4}{3}$ | $\frac{1}{4}$ | | |
| 5 | $\frac{137}{60}$ | -5 | 5 | $-\frac{10}{3}$ | $\frac{5}{4}$ | $-\frac{1}{5}$ | |
| 6 | $\frac{147}{60}$ | -6 | $\frac{15}{2}$ | $-\frac{20}{3}$ | $\frac{15}{4}$ | $-\frac{6}{5}$ | $\frac{1}{6}$ |

known that the BDF2 is *A-stable* and higher-order BDFs are not. Therefore, the second-

order scheme is unconditionaly stable, but higher-order BDFs are conditionally stable. Consequently, the stability of the higher-order schemes depends on the spatial discretization. Estimates for the maximum-allowable CFL numbers are given in Appendix A for a set of representative high-order schemes developed in this paper.

Towards the pseudo steady state, the variable $p$ approaches the solution gradient and hence the above equation becomes identical to the original advection-diffusion equation with the time derivative discretized by the BDF, i.e., a consistent discretization of the original equation. The system reduces, of course, to the original steady equation also in the physical steady state when $\partial_t u = 0$. Second-order accurate unsteady computations have been demonstrated based on the above formulation in Ref. [6].

In the vector form, our time-dependent first-order advection-diffusion system can be written as

$$\frac{\partial \mathbf{U}}{\partial \tau} + \mathbf{A}\frac{\partial \mathbf{U}}{\partial x} = \mathbf{S}, \tag{4}$$

where

$$\mathbf{U} = \begin{bmatrix} u \\ p \end{bmatrix}, \quad \mathbf{A} = \begin{bmatrix} a & -\nu \\ -1/T_r & 0 \end{bmatrix}, \quad \mathbf{S} = \begin{bmatrix} -\alpha u/\Delta t + S(x) \\ -p/T_r \end{bmatrix}. \tag{5}$$

For any positive $T_r$, the Jacobian has the following two real eigenvales:

$$\lambda_1 = \frac{a}{2}\left[1 - \sqrt{1 + \frac{4\nu}{a^2 T_r}}\right], \quad \lambda_2 = \frac{a}{2}\left[1 + \sqrt{1 + \frac{4\nu}{a^2 T_r}}\right], \tag{6}$$

with linearly independent eigenvectors [6], and therefore the above system is hyperbolic in the pseudo time. The hyperbolicity serves mainly as a guide for discretization: various discretization techniques are available for hyperbolic systems, e.g., upwinding. In addition to the convenience in discretization, the major benefits are: 1) the hyperbolic discretization results in a strong coupling between the two variables that results in the equal order of accuracy for both $u$ and $p = \partial_x u$ on arbitrary grids, and 2) $O(1/h)$ acceleration is achieved in iterative convergence for the linearized residual equation in implicit solvers due to the $O(1/h)$ condition number of the Jacobian, which is $O(h)$ smaller than that of the Jacobian derived from a conventional diffusion scheme. For explicit schemes, the $O(1/h)$ acceleration is achieved by the $O(h)$ time step typical in methods for hyperbolic systems, which is $O(1/h)$ times larger than a typical time step of $O(h^2)$ for diffusion. The $O(1/h)$ acceleration in convergence has been demonstrated over traditional methods for the diffusion equation [1, 4], for the advection-diffusion equation [2, 5], for the compressible Navier-Stokes equations [3],

and most recently for time-dependent linear and nonlinear advection-diffusion problems using RD technique [6].

In the next sections, we first briefly describe the second-order time-dependent discretization process using the RD scheme. Further details are given in Ref. [6]. We then extend the order of accuracy of the scheme to third-order and fourth-order RD hyperbolic advection-diffusion schemes with reformulation of the hyperbolic system, and finally to higher order (fourth- and sixth-order) RD hyperbolic advection-diffusion schemes with introduction of new source term discretization technique.

## 3. Second-Order RD Hyperbolic Advection-Diffusion

The RD method requires 1) evaluation of the cell (or element) residuals, and 2) the distribution of the residuals to the nodes bounding the cell. Consider a one-dimensional domain discretized with $N$ nodes that are distributed arbitrary over the domain of interest with the solution, $u$, and the solution gradient, $p = \partial_x u$, data stored at the nodes denoted by $x_i$, $i = 1, 2, 3, ..., N$ (Fig.1). We define the cell-residual $\mathbf{\Phi^C}$ by integrating the spatial part

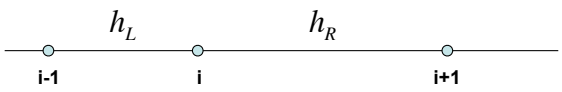


Figure 1: Schematic of grid spacing for a 1-D grid.

of the Eq. (4) over the cell, $C$, defined by the nodes $i$ and $i+1$:

$$\Phi^C = \int_{x_i}^{x_{i+1}} (-\mathbf{A}\mathbf{U}_x + \mathbf{S}) dx, \tag{7}$$

$$= \begin{cases} -a(u_{i+1} - u_i) + \nu(p_{i+1} - p_i) \\ \\ \dfrac{1}{T_r}\left[u_{i+1} - u_i\right] \end{cases} + \int_{x_i}^{x_{i+1}} \mathbf{S}\ dx. \tag{8}$$

The first term of the Eq. (8) is the result of the exact integration of $-\mathbf{A}\mathbf{U}_x$ over the cell $C$. The integration of the second term is not exact and therefore is the source of the overall discretization error. We will further discuss this discretization error in the following sections.

We construct the spatial discretization of Eq. (4) by distributing the cell residuals to the nodes:

$$\frac{d\mathbf{U}_i}{d\tau} = \frac{1}{h_i}(B^+\Phi^L + B^-\Phi^R), \tag{9}$$

where $\Phi^L$ and $\Phi^R$ denote the cell-residuals over the left and right cells of the node $i$, respectively, and $h_i$ is the dual volume (see Fig. 1) defined by

$$h_i = \frac{h_L + h_R}{2}, \quad h_L = x_i - x_{i-1}, \quad h_R = x_{i+1} - x_i. \tag{10}$$

Note that the pseudo time derivative on the left hand side is retained here just for the sake of illustration. It will be ignored in the implicit formulation that follows. Our aim is to directly solve it for the pseudo steady state, which corresponds to the next physical time. In this sense, our method is not a dual-time stepping method. The distribution matrices $B^-$ and $B^+$ (Fig. 2) typically do not affect the order of accuracy of the discretization scheme; it is determined by the cell-residuals [22, 23], and therefore our focus will be on the residual evaluation. (Refer to Ref. [6] for formulation of the distribution matrices $B^-$ and $B^+$).

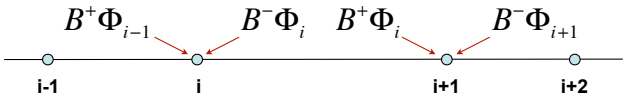


Figure 2: Residual distribution to the nodes.

### *3.1. Second-Order Discretization*

We may use a simple trapezoidal rule for the integration of the source term $\mathbf{S}$ over the cell $C$ and arrive at the following cell residuals:

$$\Phi^C = \begin{bmatrix} -a(u_{i+1} - u_i) + \nu(p_{i+1} - p_i) - (x_{i+1} - x_i)\dfrac{\alpha}{\Delta t}(u_{i+1} + u_i)/2 \\ \\ (u_{i+1} - u_i - (x_{i+1} - x_i)(p_{i+1} + p_i)/2)/T_r \end{bmatrix}^{k+1}$$

$$+ \begin{bmatrix} (x_{i+1} - x_i)(\tilde{s}_{i+1} + \tilde{s}_i)/2 \\ \\ 0 \end{bmatrix}^{n-1,n}, \tag{11}$$

where $k$ and $n$ are the Newton iteration counter (as described below) and the physical time index, respectively. Note that the second term of the Eq. (11), which is computed at the two previous physical time steps, is constant during the Newton iteration, and thus will not contribute to the Jacobian.

The implicit formulation is defined by

$$\mathbf{U}^{k+1} = \mathbf{U}^k + \Delta\mathbf{U}^k, \tag{12}$$

where $\mathbf{U} = (u_1, p_1, u_2, p_2, \ldots, u_N, p_N)$ and $k$ is the iteration counter. The correction $\Delta\mathbf{U}^k = \mathbf{U}^{k+1} - \mathbf{U}^k$ is determined as the solution to the linear system:

$$\frac{\partial \mathbf{Res}}{\partial \mathbf{U}} \Delta\mathbf{U}^k = -\mathbf{Res}^k, \tag{13}$$

where $\mathbf{Res}^k$ is the right hand side of Equation (9), which is the unsteady residual vector evaluated by $\mathbf{U}^k$. Note that the pseudo time derivative has been ignored. The Jacobian matrix is sparse, having three 2×2 blocks in each row for all interior nodes and two blocks for boundary nodes. The $i$-th pair of rows of the linear system is given by

$$J_{i-1}\Delta U_{i-1}^k + J_i \Delta U_i^k + J_{i+1}\Delta U_{i+1}^k = -\frac{1}{h_i}(B^+\Phi^L + B^-\Phi^R)^k, \tag{14}$$

where $\Delta U_{i-1}^k = (\Delta u_{i-1}^k, \Delta p_{i-1}^k)$, $\Delta U_i^k = (\Delta u_i^k, \Delta p_i^k)$, $\Delta U_{i+1}^k = (\Delta u_{i+1}^k, \Delta p_{i+1}^k)$,

$$J_{i-1} = \frac{1}{h_i}\frac{\partial(B^+\Phi^L)}{\partial U_{i-1}}, \tag{15}$$

$$J_i = \frac{1}{h_i}\left(\frac{\partial(B^+\Phi^L)}{\partial U_i} + \frac{(\partial B^-\Phi^R)}{\partial U_i}\right), \tag{16}$$

$$J_{i+1} = \frac{1}{h_i}\frac{\partial(B^-\Phi^R)}{\partial U_{i+1}}. \tag{17}$$

We note that the derivative of the distribution matrices, $B^-$ and $B^+$, are zero for linear advection-diffusion problems and for nonlinear problems with constant $a/\nu$ values, which, for simplicity, are the only nonlinear system considered in this paper. However, the proposed schemes are applicable to general nonlinear advection-diffusion problems.

The residual Jacobians needed in the Newton solver are exactly in the same form as the above equations, but the derivatives of the cell-residuals now include the contribution from the physical time derivative:

$$\frac{\partial \Phi_R}{\partial U_i} = \begin{bmatrix} a - h_R\dfrac{\alpha}{2\Delta t} & -\nu \\ -\dfrac{1}{Tr} & -\dfrac{h_R}{2T_r} \end{bmatrix}, \tag{18}$$

$$\frac{\partial \Phi_L}{\partial U_i} = \begin{bmatrix} -a - h_L\dfrac{\alpha}{2\Delta t} & \nu \\ \dfrac{1}{Tr} & -\dfrac{h_L}{2T_r} \end{bmatrix}. \tag{19}$$

At each physical time level $n$, we solve the pseudo steady problem by Newton's method with the current solution at $n$ as the initial solution. This results in second-order discretization, which was demonstrated with several examples (linear and nonlinear) in Ref. [6].

We now focus on the truncation error of the source term discretization as it is needed for our discussion in the next sections where we show two different approaches to obtain higher-order RD schemes. We demonstrate the truncation error of the system by considering the residual of the second equation in our hyperbolic advection-diffusion system:

$$\Phi_p^C = (u_{i+1} - u_i - h(p_{i+1} + p_i)/2)/T_r, \tag{20}$$

where $h$ is the width of the cell $C$ (i.e. $x_{i+1} - x_i$). We now expand the $\Phi_p^C$ around the node $i$ to obtain the truncation error ($T.E.$) for the second equation, $\partial_\tau p$, which after some algebra and rearrangements becomes:

$$\begin{aligned} T.E.\ (\partial_\tau p) &= \left[(\partial_x u_i - p_i) + \frac{h}{2}(\partial_{xx} u_i - \partial_x p_i) + \frac{h^2}{6}(\partial_{xxx} u_i - \frac{6}{4}\partial_{xx} p_i) + O(h^3)\right]/T_r \\ &= O(h^2), \end{aligned} \tag{21}$$

where the first two terms will simply vanish as they satisfy the original equation in the pseudo steady state. The non-vanishing last term makes the current discretization second-order. The same results are obtained with the first equation and therefore is not repeated here. The above analysis shows that the error arises from the source term discretization, not from the flux balance term, which is exact in one dimension. It implies that we can achieve high-order accuracy only by improving the source term discretization. In fact, in Ref.[14], a fourth-order finite-difference scheme is constructed in this manner, i.e., by a high-order source term discretization with explicit pseudo-time stepping targeted for steady problems.

Note that the above truncation error analysis is based on the cell-residual expanded at a node. Hence, the nodal residual has the same order as the cell-residuals because it is constructed as a weighted sum of the cell-residuals as shown in Eq. (9). Note also that the truncation error analysis based on the cell-residual is local to the cell and thus valid for any size of the cell, i.e., valid for uniform and nonuniform grids. In the rest of the paper, the truncation error analysis is all based on the cell-residual.

In the next sections, we show two different techniques that will lead to higher-order schemes. In particular, we discuss on 1) reformulation of the source term with its divergence form, and 2) new source term discretization technique which acts as a correction to the trapezoidal rule.

## 4. High-Order RD Scheme with Source Term Reformulation (Third- & Fourth-Order)

Consider the source term, $S$, as the divergence of a function $f^S$: $f^S_x = S$. We now replace the source terms with their divergence forms, and rewrite our first-order hyperbolic advection-diffusion equation as

$$\begin{aligned} \partial_\tau u &= -a\,\partial_x u + \nu\,\partial_x p + \partial_x f^S_u, && (22)\\ \partial_\tau p &= (\partial_x u - \partial_x f^S_p)/T_r, && (23) \end{aligned}$$

where $f^S_u$ and $f^S_p$ are the divergence formulation of the source terms in the $u$ and the $p$ equations, respectively. With the above reformulation of the advection-diffusion equation, which will be discussed in more details, the residual evaluations of the system becomes exact with no special discretization scheme:

$$\begin{aligned} \tilde{\Phi}^C &= \int_{x_i}^{x_{i+1}} (-\mathbf{A}\mathbf{U}_x + \mathbf{f}^S_x)dx, && (24)\\ &= \begin{cases} -a(u_{i+1}-u_i) + \nu(p_{i+1}-p_i) + (f^S_u)_{i+1} - (f^S_u)_i \\ \dfrac{1}{T_r}\left[u_{i+1} - u_i - (f^S_p)_{i+1} + (f^S_p)_i\right] \end{cases}. && (25) \end{aligned}$$

We remark that even though the residual evaluation of our reformulated advection-diffusion system is exact, the overall accuracy of the scheme depends on the accuracy of the divergence formulation of the source terms and how it is formulated.

### *4.1. Third-Order Scheme with Divergence Form*

Following the divergence formulation introduced in [8], we write the source flux in a more general form:

$$\begin{aligned} f^S &= \sum_{n=1}^{m\geq 3} \frac{(-1)^{n-1}}{n!}(x-x_i)^n \partial_{x^{n-1}} S, && (26)\\ &= (x-x_i)S - \frac{1}{2}(x-x_i)^2\partial_x S + \frac{1}{6}(x-x_i)^3\partial_{xx}S - \frac{1}{24}(x-x_i)^4\partial_{xxx}S + \ldots, && (27) \end{aligned}$$

where the source term $S$ and its derivatives $S_x$, $S_{xx}$, etc. are not constants but functions that vary in space. We remark that the source flux, $f^S$, is not necessarily a polynomial of order $m$ because it depends on the derivatives of the source term $S$. In this paper, we do

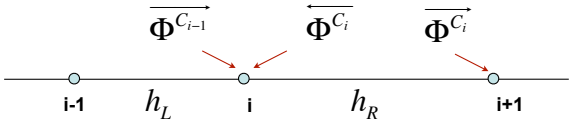


Figure 3: Cell residual evaluation with divergence form of the source term.

not consider high-order schemes that require evaluation of third or higher derivatives. The divergence of the source flux, $\partial_x f^S$, for the third-order accuracy (i.e. $m = 3$) is

$$\partial_x f^S = S + \frac{h^3}{6}\partial_{xxx} S = S + O(h^3), \tag{28}$$

which is identical to the original equation up to the third-order. We remark that this error does not necessarily limit the maximum order attained by numerical schemes. In the next section, we will show that a fourth-order scheme can be constructed by a slightly modified divergence form with $m = 3$.

Discretization of the reformulated hyperbolic system leads to the cell residual, for example, for the second equation as

$$\Phi_p^C = \left[u_{i+1} - u_i - (f_p^S)_{i+1} + (f_p^S)_i\right]/T_r, \tag{29}$$

where special care must be taken when we evaluate $f_i^S$ and $f_{i+1}^S$ (because of the presence of $x_i$ in the divergence formulation) as they depend on whether the cell residual is being distributed to the left or to the right node of the cell (Fig. 3):

$$\begin{aligned}
\overleftarrow{\Phi_p^{C_i}} &= \left[u_{i+1} - u_i - (f_p^S)_{i+1} + (f_p^S)_i\right]/T_r, \\
&= \left[u_{i+1} - u_i - h_R S_{i+1} + \frac{h_R^2}{2}\partial_x S_{i+1} - \frac{h_R^3}{6}\partial_{xx} S_{i+1}\right]/T_r, \qquad (30) \\
\overrightarrow{\Phi_p^{C_i}} &= \left[u_{i+1} - u_i - (f_p^S)_{i+1} + (f_p^S)_i\right]/T_r, \\
&= \left[u_{i+1} - u_i + h_R S_i + \frac{h_R^2}{2}\partial_x S_i + \frac{h_R^3}{6}\partial_{xx} S_i\right]/T_r. \qquad (31)
\end{aligned}$$

The source term discretization is, therefore, not conservative, which is natural and appropriate because the source term does not have a conservative property and should not be discretized in such a way. If it is conservative, the global sum of the cell-residual for the source term will depend only on the boundary data (telescoping property), which is wrong for the source term.

We now show that the truncation error ($T.E.$) of the resulting RD scheme with the above divergence formulation of the source term (with $m = 3$) is in fact third-order. Again, for

demonstration purposes we consider the second equation (i.e. $\partial_\tau p$); the same process can be repeated for the first equation. We first expand the source fluxes around the node $i$:

$$\int_{x_i}^{x_{i+1}} \partial_x f^S dx = f^S_{i+1} - f^S_i = h_R \partial_x f^S + \frac{h_R^2}{2}\partial_{xx} f^S + \frac{h_R^3}{6}\partial_{xxx} f^S + O(h^4), \tag{32}$$

where the $\partial_x f^S$ is given by Eq. (28), and

$$\partial_{xx} f^S = \partial_x S + \frac{h_R^2}{2}\partial_{xxx} S + \frac{h_R^3}{6}\partial_x^{(4)} S + O(h^4), \tag{33}$$

$$\partial_{xxx} f^S = \partial_{xx} S + h_R \partial_{xxx} S + h_R^2 \partial_x^{(4)} S + \frac{h_R^3}{6}\partial_x^{(5)} S + O(h^4). \tag{34}$$

Using Eq. (29), we evaluate the truncation error of the equation $\partial_\tau p$ by substituting Eqs. (33) and (34) into Eq. (32) and expanding all the terms in Eq. (29) around the node $i$:

$$\begin{aligned} T.E.\ (\partial_\tau p) &= \left[(\partial_x u_i - p_i) + \frac{h_R}{2}(\partial_{xx} u_i - \partial_x p_i) + \frac{h_R^2}{6}(\partial_{xxx} u_i - \partial_{xx} p_i)\right]/T_r \\ &+ \left[\frac{h_R^3}{24}(\partial_x^{(4)} u_i - 14\,\partial_{xxx} p_i) + O(h^4)\right]/T_r \\ &= 0 + O(h^3), \end{aligned} \tag{35}$$

where the first three terms vanish as they satisfy our original equation. The presence of the last term confirms that the proposed divergence formula with $m = 3$ makes our scheme third-order accurate. The same result is obtained for the first equation with the divergence formulation of the corresponding source terms, and therefore the process is not repeated here.

We remark that the cost of this new third-order accurate RD hyperbolic advection-diffusion scheme using the divergence formulation of the source terms is only the evaluation of the first and second derivatives of the source terms; i.e., $\partial_x S$ and $\partial_{xx} S$. Note that the source flux is third-order accurate (see Eq. 28). Thus, according to the Eqs. (30) and (31), we need second-order and first-order accurate discretization for $\partial_x S$ and $\partial_{xx} S$, respectively. We derive these discretization by fitting a quadratic function through the node $i$ and its two neighbors $i-1$ and $i+1$ to arrive (after some algebra) at the following formulas that are applicable to the internal nodes of general arbitrary grids (uniform and nonuniform):

$$\partial_x S_i = \frac{-h_R^2 S_{i-1} + (h_R^2 - h_L^2) S_i + h_L^2 S_{i+1}}{h_R h_L (h_R + h_L)} + O(h^2), \tag{36}$$

$$\partial_{xx} S_i = \frac{h_R S_{i-1} - (h_R + h_L) S_i + h_L S_{i+1}}{h_R h_L (h_R + h_L)/2} + O(h), \tag{37}$$

where $h_R$ and $h_L$ are defined in Eq. (10). The corresponding one-sided formulas for the boundary nodes of general arbitrary grids are

$$\partial_x S_1 = \frac{-h_{L^*}(h_{L^*}+2h_R)S_1 + (h_R+h_{L^*})^2 S_2 - h_R^2 S_3}{h_R h_{L^*}(h_R+h_{L^*})} + O(h^2), \tag{38}$$

$$\partial_x S_N = \frac{h_L(h_L+2h_{R^*})S_N - (h_{R^*}+h_L)^2 S_{N-1} + h_{R^*}^2 S_{N-2}}{h_{R^*} h_L(h_{R^*}+h_L)} + O(h^2), \tag{39}$$

$$\partial_{xx} S_1 = \frac{h_{L^*} S_1 - (h_R+h_{L^*})S_2 + h_R S_3}{h_R h_{L^*}(h_R+h_{L^*})/2} + O(h), \tag{40}$$

$$\partial_{xx} S_N = \frac{-h_{R^*} S_N + (h_{R^*}+h_L)S_{N-1} - h_L S_{N-2}}{h_{R^*} h_L(h_{R^*}+h_L)/2} + O(h), \tag{41}$$

where $h_{L^*}$ and $h_{R^*}$ are defined as

$$h_{L^*} = x_3 - x_2, \quad h_{R^*} = x_{N-1} - x_{N-2}. \tag{42}$$

It is clear from the above formulas that each derivative can be computed in a three-point stencil. Consequently, the residual at a node is defined in a five-point stencil in the interior, a four-point stencil at the nodes adjacent to the boundary, and a three-point stencil at the boundary nodes. In the next section, we demonstrate that a fourth-order scheme can be constructed without extending the stencil.

### *4.2. Fourth-Order Scheme with Divergence Form*

Here, we show how a simple modification to the presented divergence form upgrades the scheme order by one order; that is our third-order scheme becomes fourth-order with no additional cost. To gain an order, we propose the divergence form of the source terms with

$$f^S = \sum_{n=1}^{m\geq 3} \frac{(-1)^{n-1}}{n!}(x-\bar{x})^n \partial_{x^{n-1}} S, \tag{43}$$

$$= (x-\bar{x})S - \frac{1}{2}(x-\bar{x})^2\partial_x S + \frac{1}{6}(x-\bar{x})^3\partial_{xx} S - \frac{1}{24}(x-\bar{x})^4\partial_{xxx} S + \ldots, \tag{44}$$

where $\bar{x} = (x_i + x_{i+1})/2$. Note that the previous divergence form was formed around the $x_i$ while this new formulation defines the divergence function around the mid-point $\bar{x}$. Similar to the divergence form presented in the previous section, the source term and its derivatives are not constants but functions that vary in space. And therefore, when the source flux is differentiated it recovers the original source term up to $O(h^m)$ around the node $i$. For $m = 3$, we have:

$$\partial_x f^S = S + \frac{(x-\bar{x})^3}{6}\partial_{xxx} S = S + O(h^3). \tag{45}$$

Again, it does not limit the maximum order of accuracy for numerical schemes, and it is possible to construct even higher-order schemes.

We now show that this third-order source divergence formulation will result in a fourth-order accurate RD scheme. We do this similarly to the process explained in the previous section except that the second and third derivatives of the $f^S$ are now defined as:

$$\partial_{xx} f^S = \partial_x S + \frac{(x-\bar{x})^2}{2}\partial_{xxx} S + \frac{(x-\bar{x})^3}{6}\partial_x^{(4)} S + O(h^4), \tag{46}$$

$$\partial_{xxx} f^S = \partial_{xx} S + (x-\bar{x})\partial_{xxx} S + (x-\bar{x})^2\partial_x^{(4)} S + \frac{(x-\bar{x})^3}{6}\partial_x^{(5)} S + O(h^4). \tag{47}$$

Again, for discussion purposes, we consider the second equation of the hyperbolic advection-diffusion system, $\partial_\tau p$. The truncation error of the $p$ equation after substituting Eqs. (46) and (47) into Eq. (32) becomes:

$$\begin{aligned} T.E.\ (\partial_\tau p) &= \left[(\partial_x u_i - p_i) + \frac{h_R}{2}(\partial_{xx} u_i - \partial_x p_i) + \frac{h_R^2}{6}(\partial_{xxx} u_i - \partial_{xx} p_i)\right]/T_r \\ &+ \left[\frac{h_R^3}{24}(\partial_x^{(4)} u_i - \partial_{xxx} p_i) + \frac{h_R^4}{120}(\partial_x^{(5)} u_i - \frac{5}{4}\partial_x^{(4)} p_i) + O(h^5)\right]/T_r \\ &= 0 + O(h^4), \end{aligned} \tag{48}$$

which is fourth-order accurate because of the cancellation of the first four terms of the truncation error equation. Another great property of this new divergence formulation is the equal evaluation of the $f_{i+1}^S - f_i^S$ regardless of whether the source flux is being transferred to the node $i$ or $i+1$. This greatly simplifies the implementation of this form of divergence formulation.

Note that the identical residual is distributed to the left and right nodes in this scheme. It then appears that the source term discretization is conservative. However, it is actually not conservative for the source term because the cell-residual for the source term depends on the coordinate of the mid-point of the cell and thus it is not telescoping. Again, this is natural and appropriate for the source term, which has no conservation property and should be local.

## 5. Higher-Order RD Scheme with Generalized Trapezoidal Rule (Third-, Fourth- & Sixth-order)

In the previous section, we reformulated the original hyperbolic advection-diffusion system with a generalized divergence form of the source terms and arrived at third- and fourth-order RD schemes. We specifically showed that both the third- and the fourth-order RD

schemes developed with the divergence formulation of the source terms require the evaluation of the first and second derivatives of the source terms. Fifth- and higher-order schemes can be systematically constructed with the divergence formulation, but may require the evaluation of third- and higher-order derivatives that would extend the stencil to the neighbors of the neighbors and beyond. From a practical point of view, such high-order schemes are not very attractive, and thus not considered here.

In this section, we introduce a different technique to develop even higher-order schemes without the need to evaluate gradients beyond the second-derivatives. We also show that with this new technique the fourth-order RD scheme is even less computationally intensive than the third- and fourth-order RD schemes that are developed with the divergence formulation of the source terms.

Consider the vector form of our first-order hyperbolic advection-diffusion system:

$$\frac{\partial \mathbf{U}}{\partial \tau} + \mathbf{A}\frac{\partial \mathbf{U}}{\partial x} = \mathbf{S}. \tag{49}$$

We showed in Section 3 that the source term discretization with the trapezoidal rule provides a second-order accurate scheme. This trapezoidal rule can be written as

$$\int_i^{i+1} S dx = \frac{h_R}{2}(S_L + S_R), \tag{50}$$

where for the second-order scheme $S_L = S_i$ and $S_R = S_{i+1}$; i.e., the arithmetic averaging of the source terms between the left and the right nodes (Fig. 4). Generalizing the trapezoidal rule, we propose the following formula for the left and right source terms, $S_L$ and $S_R$ respectively:

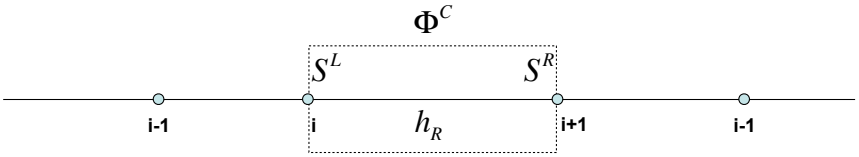


Figure 4: Source term discretization.

$$S_L = S_i + C_1^L \partial_x S_i + C_2^L \partial_{xx} S_i, \tag{51}$$

$$S_R = S_{i+1} + C_1^R \partial_x S_{i+1} + C_2^R \partial_{xx} S_{i+1}, \tag{52}$$

where $C_1^L$ and $C_1^R$ are constants of $O(h)$, and $C_2^L$ and $C_2^R$ are of $O(h^2)$. A somewhat similar approach is taken in Ref. [15], introduced for upgrading the order of accuracy of a finite-volume scheme, where not only the source term but also the interface flux need to be modified

for high-order accuracy. We find these constants by making sure that the nodal residuals of the two equations in our hyperbolic system are accurate up to the desired order of accuracy of the scheme we are seeking to develop. With the above equation, the maximum possible order of accuracy is six. We also note that the fifth-order RD scheme with the above proposed source term discretization becomes mathematically sixth-order.

### *5.1. Third-Order RD Scheme with Generalized Trapezoidal Rule*

A third-order RD scheme can be obtained if the coefficients of the proposed discretization formulation satisfy the following equations:

$$C_1^L + C_1^R = 0, \quad C_1^R h_R + C_2^L + C_2^R = -\frac{h_R^2}{6}, \quad C_1^R h_R + 2C_2^R \neq -\frac{h_R^2}{6}, \tag{53}$$

which can be derived from the truncation error analysis. Here, there are four unknowns for three equations; thus there are infinite combinations with the $C_1^R$ as a free parameter. We also note that there is no relation between this third-order RD scheme and the third-order scheme developed with the divergence formulation; the nodal residual of the source terms obtained with the previous third-order scheme depends only on the information from its immediate node neighbor and not the node itself. On the other hand, the new third-order RD scheme that is developed with a correction to the trapezoidal rule depends both on its immediate node neighbor and the node itself. Consequently, it is not possible to reproduce the previous third-order scheme by any choice of the coefficients. Note, however, that this scheme has the same stencil with the previous third-order scheme: a five-point stencil in the interior, a four-point stencil at the nodes adjacent to the boundary, and a three-point stencil at the boundary nodes. The same is true for the fourth-order scheme derived in the next section.

Assuming $C_1^R = -h_R/6$, the left and right source functions of the source discretization may be chosen as:

$$S_L = S_i + \frac{h_R}{6}\partial_x S_i, + \frac{h_R^2}{1000}\partial_{xx} S_i \tag{54}$$

$$S_R = S_{i+1} - \frac{h_R}{6}\partial_x S_{i+1} - \frac{h_R^2}{1000}\partial_{xx} S_{i+1}. \tag{55}$$

We can now evaluate the truncation error of the hyperbolic advection-diffusion system. Here we show the truncation error of the second equation; the same will be true for the first equation as well. The cell residual of the second equation with the third-order RD scheme

with the generalized trapezoidal rule is:

$$\begin{aligned}\Phi_u^C &= -a(u_{i+1}-u_i)+\nu(p_{i+1}-p_i)+\frac{h_R}{2}(S_L+S_R),\\ &= -a(u_{i+1}-u_i)+\nu(p_{i+1}-p_i)+\frac{h_R}{2}(S_{i+1}+S_i)\\ &- \frac{h_R^2}{12}(\partial_x S_{i+1}-\partial_x S_i)-\frac{h_R^3}{2000}(\partial_{xx}S_{i+1}-\partial_{xx}S_i).\end{aligned} \tag{56}$$

We then expand the cell residual around the node i to arrive at the following truncation error:

$$\begin{aligned}T.E.(\partial_\tau u_i) &= (-a\partial_x u_i+\nu\partial_x p_i+S_i)+\frac{h_R}{2}(-a\partial_{xx}u_i+\nu\partial_{xx}p_i+\partial_x S_i)\\ &+ \frac{h_R^2}{6}(-a\partial_{xxx}u_i+\nu\partial_{xxx}p_i+\partial_{xx}S_i)\\ &+ \frac{h_R^3}{24}(-a\partial_x^{(4)}u_i+\nu\partial_x^{(4)}p_i+0.988\,\partial_{xxx}S_i)+O(h^4)\\ &= 0+O(h^3),\end{aligned} \tag{57}$$

where the first three terms vanish but the last term makes the scheme third-order accurate. As we will show next, smaller values for the coefficients $C_2^R$ or $C_2^L$ move the schemes to fourth-order accurate. This is further shown in the following section.

### *5.2. Fourth-Order RD Scheme with Generalized Trapezoidal Rule*

Fourth-order accuracy is achievable by a simple adjustment to the condition given in Eq. (53):

$$C_1^L+C_1^R=0,\quad C_1^R h_R+C_2^L+C_2^R=-\frac{h_R^2}{6},\quad \frac{C_1^R}{2}h_R+C_2^R=-\frac{h_R^2}{12}. \tag{58}$$

Again, the coefficients cannot be determined uniquely, and there are many solutions. A particularly interesting solution is the following:

$$C_1^L=+\frac{h_R}{6},\quad C_2^L=0,\quad C_1^R=-\frac{h_R}{6},\quad C_2^R=0. \tag{59}$$

As will be shown shortly, it leads to a fourth-order RD scheme with the source term discretization by Eqs. (51) and (52):

$$S_L = S_i+\frac{h_R}{6}\partial_x S_i, \tag{60}$$

$$S_R = S_{i+1}-\frac{h_R}{6}\partial_x S_{i+1}, \tag{61}$$

It is remarkable that the fourth-order scheme does not require the evaluation of the second derivatives and is thus less expensive than the third-order schemes developed in the previous

sections. It is, of course, possible to develop a fourth-order RD scheme with addition of the second derivatives in the source term discretization. For example the following constants will also result in a fourth-order RD scheme:

$$C_1^L = +\frac{h_R}{4}, \quad C_2^L = +\frac{h_R}{24} \quad C_1^R = -\frac{h_R}{4}, \quad C_2^R = +\frac{h_R}{24}, \tag{62}$$

which makes this fourth-order RD scheme identical to the fourth-order RD scheme constructed by the divergence formulation in Section 4.2. Although it is possible to construct, these fourth-order schemes are not very attractive as they require second derivatives of the source term, and therefore not considered in this paper.

We now prove the fourth-order accuracy of the scheme by evaluating the cell residual of, for example, the first equation; i.e. $\Phi_u^C$:

$$\begin{aligned} \Phi_u^C &= -a(u_{i+1} - u_i) + \nu(p_{i+1} - p_i) + \frac{h_R}{2}(S_L + S_R), \\ &= -a(u_{i+1} - u_i) + \nu(p_{i+1} - p_i) + \frac{h_R}{2}(S_{i+1} + S_i) - \frac{h_R^2}{12}(\partial_x S_{i+1} - \partial_x S_i). \end{aligned} \tag{63}$$

Expanding the cell residual around the node $i$, we obtain the truncation error of the first equation (after some algebra) as

$$\begin{aligned} T.E.(\partial_\tau u_i) &= (-a\partial_x u_i + \nu\partial_x p_i + S_i) + \frac{h_R}{2}(-a\partial_{xx} u_i + \nu\partial_{xx} p_i + \partial_x S_i) \\ &+ \frac{h_R^2}{6}(-a\partial_{xxx} u_i + \nu\partial_{xxx} p_i + \partial_{xx} S_i) \\ &+ \frac{h_R^3}{24}(-a\partial_x^{(4)} u_i + \nu\partial_x^{(4)} p_i + \partial_{xxx} S_i) \\ &+ \frac{h_R^4}{120}(-a\partial_x^{(5)} u_i + \nu\partial_x^{(5)} p_i + \frac{5}{6}\partial_x^{(4)} S_i) + O(h^5) \\ &= 0 + O(h^4), \end{aligned} \tag{64}$$

where the first four terms of the above equation vanish (because of consistency relations). Similar conclusion is obtained for the second equation and therefore it is not repeated here. Also, note that the accuracy is achieved for general arbitrary grids. The additional cost of upgrading the second-order scheme to the fourth-order RD scheme is only due to the evaluation of the second-order accurate first derivative of the source terms. The general second-order accurate first derivative formulation for arbitrary grids is provided in Sec. 3.1.

### *5.3. ~~Fifth-order~~ & Sixth-Order RD Scheme with Generalized Trapezoidal Rule*

In this section, we present a new sixth-order RD scheme with relatively similar cost to our newly introduced third-order RD schemes. Specifically, we show that there exists a

unique fifth-order RD scheme with the generalized trapezoidal rule, and that mathematically becomes sixth-order RD scheme. Seeking fifth-order accuracy from the fourth-order RD scheme given in Eq. (58), we find an additional constraint:

$$\frac{C_1^R}{3}h_R + C_2^R = -\frac{h_R^2}{20}. \tag{65}$$

Then, the number of constraints (four) matches the number of unknown coefficients (four). In this case, therefore, there exists a unique solution:

$$C_1^L = +\frac{h_R}{5}, \quad C_2^L = +\frac{h_R^2}{60}, \quad C_1^R = -\frac{h_R}{5}, \quad C_2^R = +\frac{h_R^2}{60}. \tag{66}$$

Interestingly, the above unique coefficients satisfy the following constraint as well, which is the requirement for sixth-order accuracy:

$$\frac{C_1^R}{4}h_R + C_2^R = -\frac{h_R^2}{30}. \tag{67}$$

Thus, we have developed a sixth-order RD scheme with the generalized trapezoidal rule. We remark that these coefficients, unlike the ones proposed for the third-order and fourth-order schemes, are unique. With the proposed constants for the sixth-order RD scheme, the source term evaluations at the nodes $i$ and $i+1$ become:

$$S_L = S_i + \frac{h_R}{5}\partial_x S_i + \frac{h_R^2}{60}\partial_{xx} S_i, \tag{68}$$

$$S_R = S_{i+1} - \frac{h_R}{5}\partial_x S_{i+1} + \frac{h_R^2}{60}\partial_{xx} S_{i+1}. \tag{69}$$

Note that it requires only the first and second derivatives of the source term, and no higher-order derivatives are required.

Similar to the process explained for the fourth-order scheme, we prove the order of accuracy of the scheme using the above proposed source discretization by first evaluating the cell residual of the hyperbolic system. Consider the cell residual of, for example, the first equation ($\Phi_u^C$):

$$\begin{aligned}
\Phi_u^C &= -a(u_{i+1} - u_i) + \nu(p_{i+1} - p_i) + \frac{h_R}{2}(S_L + S_R), \\
&= -a(u_{i+1} - u_i) + \nu(p_{i+1} - p_i) \\
&+ \frac{h_R}{2}(S_{i+1} + S_i) - \frac{h_R^2}{10}(\partial_x S_{i+1} - \partial_x S_i) + \frac{h_R^3}{120}(\partial_{xx} S_{i+1} + \partial_{xx} S_i).
\end{aligned} \tag{70}$$

Expanding the cell residual around the node $i$, we obtain the truncation error of the first equation (after some algebra) as

$$T.E.(\partial_\tau u_i) = (-a\partial_x u_i + \nu\partial_x p_i + S_i) + \frac{h_R}{2}(-a\partial_{xx} u_i + \nu\partial_{xx} p_i + \partial_x S_i)$$

$$
\begin{aligned}
&+ \quad \frac{h_R^2}{6}(-a\partial_{xxx}u_i + \nu\partial_{xxx}p_i + \partial_{xx}S_i) \\
&+ \quad \frac{h_R^3}{24}(-a\partial_x^{(4)}u_i + \nu\partial_x^{(4)}p_i + \partial_{xxx}S_i) \\
&+ \quad \frac{h_R^4}{120}(-a\partial_x^{(5)}u_i + \nu\partial_x^{(5)}p_i + \partial_x^{(4)}S_i) \\
&+ \quad \frac{h_R^5}{720}(-a\partial_x^{(6)}u_i + \nu\partial_x^{(6)}p_i + \partial_x^{(5)}S_i) \\
&+ \quad \frac{h_R^6}{5040}(-a\partial_x^{(7)}u_i + \nu\partial_x^{(7)}p_i + \frac{21}{20}\partial_x^{(6)}S_i) + O(h^7) \\
&= \quad 0 + O(h^6). \qquad (71)
\end{aligned}
$$

A similar result is obtained for the second equation, and is thus omitted here, for brevity. The above truncation error analysis reveals that this powerful sixth-order RD scheme could, in practice, produce almost seventh-order accurate results, if the sixth derivative of the source term becomes small; the sixth-order term is only due to the presence of $(h_R^6/100800)\partial_x^{(6)}S_i$ in the last term of Eq. (71). We will show such interesting results in the following section.

We emphasize that the sixth-order RD scheme, similar to the third-order RD scheme, requires the evaluation of the first and second derivatives of the source terms. However, these derivatives are now required to be evaluated with higher-order accuracy. For this sixth-order RD scheme, we need third-order and second-order accurate evaluations of the first and the second derivatives of the source terms, respectively, which can be obtained by a cubic fit. This makes the developed sixth-order scheme slightly more expensive than the third-order scheme. Nevertheless, the proposed sixth-order scheme is exceptionally simple and affordable.

## 6. Results

In this section we present the results in three categories: 1) steady advection-diffusion equation for high Reynolds (or Peclet) number applications, 2) unsteady linear advection-diffusion, and 3) unsteady nonlinear advection-diffusion problems. We obtain the results with all the proposed RD schemes and compare them with the second-order RD scheme. The order of accuracy results are also compared and presented for each example.

For all cases, we employ the Newton-GS solver as described in Section 3. It is essentially Newton's method for the second-order scheme, but an approximate Newton method for higher-order schemes because the Jacobian matrix derived from the second-order scheme is used for all higher-order schemes. For unsteady problems, the same solver is used to solve the

implicit-residual equations or equivalently to compute the pseudo steady solution at every physical time step.

### *6.1. Steady Linear Advection-Diffusion*

Consider the advection-diffusion equation in $x \in (0,1)$ with $u(0) = 0$ and $u(1) = 0$:

$$\partial_t u + a\partial_x u = \nu \partial_{xx} u + s(x), \tag{72}$$

where

$$s(x) = \nu\pi^2 \sin(\pi x) + a\pi \cos(\pi x). \tag{73}$$

The above problem has a fixed analytical solution of $\sin(\pi x)$ for any advection and diffusion coefficients. We solved this problem using the hyperbolic advection-diffusion method discussed in Section 2 with the proposed high-order RD schemes (see Fig. 5. Note that we intentionally used a very coarse grid to show that the high-order schemes could produce a much more accurate solution on such a "bad" grid.) We used ranges of nonuniform grids

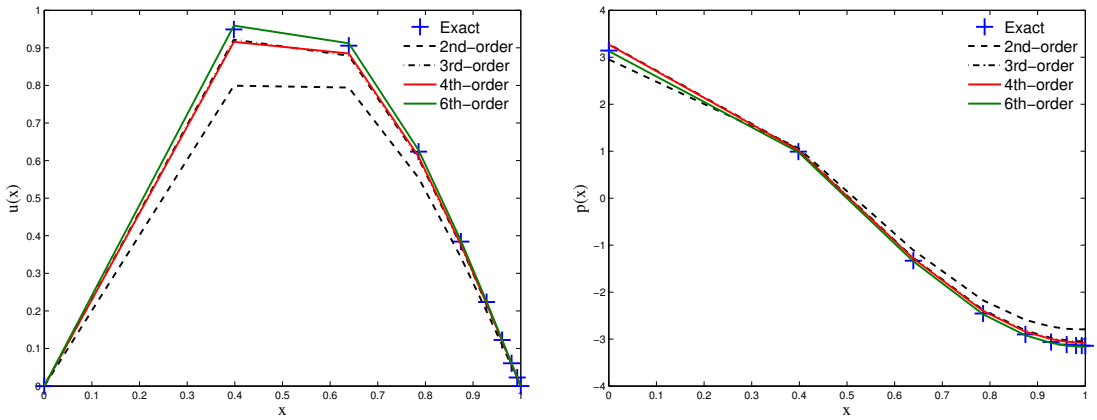


(a) $u(x)$ (b) $p(x) = du/dx$

Figure 5: Comparisons between the exact and the numerical results using the proposed high-order RD schemes for the steady linear advection-diffusion problem ($Re = 1$) on a nonuniform grid with $N = 10$.

and solved the problem with the Newton-GS method. For each Newton iteration, the GS relaxation were conducted until three orders of magnitudes reduction is achieved for the linear system. The computations were continued until the residuals of both the solution $u$ and the solution gradient $p$ were reduced by eight orders of magnitude. The convergence results are shown in Table 2, where the convergence of the GS relaxation is clearly $O(N)$ and is independent of the order of accuracy of the RD scheme. Also, the solution was converged with the same number of GS relaxations and Newton iterations regardless of the RD scheme

Table 2: Steady linear advection-diffusion problem, $Re = 1$ (Convergence criteria: Residuals $< 10^{-8}$.)

| Number of nodes | RD Scheme Order | GS relaxations/Newton iteration | | Newton iteration | |
|---|---|---|---|---|---|
| | | High-Order Technique | | High-Order Technique | |
| | | RD-D | RD-GT | RD-D | RD-GT |
| 50 | 3rd | 168 | 169 | 10 | 10 |
| | 4th | 168 | 168 | 10 | 10 |
| | 6th | – | 168 | – | 10 |
| 100 | 3rd | 325 | 325 | 8 | 8 |
| | 4th | 325 | 325 | 8 | 8 |
| | 6th | – | 325 | – | 8 |
| 200 | 3rd | 670 | 670 | 7 | 7 |
| | 4th | 670 | 670 | 7 | 7 |
| | 6th | – | 670 | – | 7 |
| 300 | 3rd | 1015 | 1015 | 7 | 7 |
| | 4th | 1015 | 1015 | 7 | 7 |
| | 6th | – | 1015 | – | 7 |
| 500 | 3rd | 1703 | 1703 | 7 | 7 |
| | 4th | 1703 | 1703 | 7 | 7 |
| | 6th | – | 1703 | – | 7 |
| 1000 | 6rd | 3416 | 3416 | 7 | 7 |
| | 4th | 3416 | 3416 | 7 | 7 |
| | 6th | – | 3416 | – | 7 |

order. Note that the solutions were converged with a very small number of Newton iterations, typically less than ten; this is exceptionally remarkable for the approximate Jacobian (second-order) formulation for higher-order schemes.

The accuracy of the proposed RD schemes were verified by computing the $L_1 = \sum_{i=1}^{N}(U_i^{exact} - U_i)/N$. These results are shown in Fig. 6 for the third-, fourth-, and sixth-order hyperbolic RD schemes (see also Tables 3, 4, and 5). Note that when the differences between the numeri-

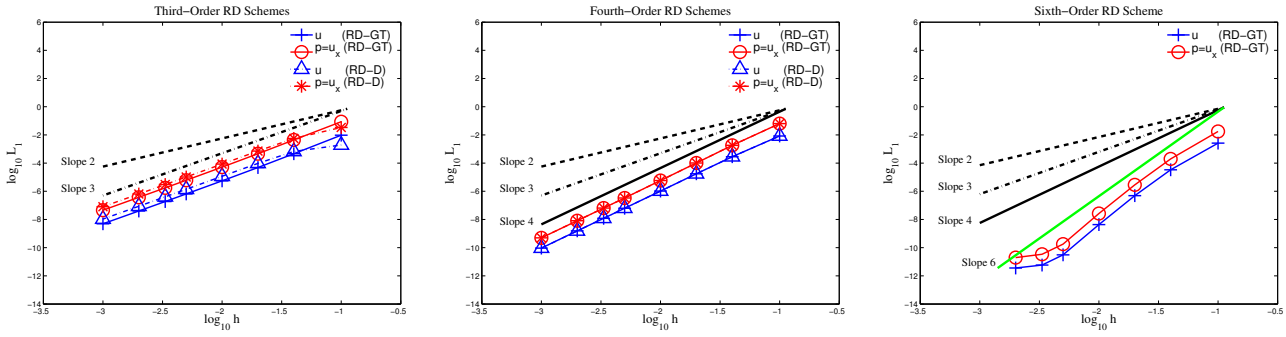


(a) third-order (b) fourth-order (c) sixth-order

Figure 6: $L_1$ error of the proposed high-order RD hyperbolic schemes for the steady linear advection-diffusion problem.

cal results and exact values approach the machine zero, the L1 slope approaches zeroth-order; these results are thus omitted from the Table 5. The RD schemes developed with the divergence formulation are denoted by *RD-D*, while the schemes developed with the generalized trapezoidal rule are denoted with *RD-GT*. The results show that all the RD schemes achieve the design order of accuracy for both the solution $u$ and the solution gradient $p$. It can be seen also that the difference between the two versions of third-order RD schemes is minor, and the same is true for the fourth-order RD schemes.

### *6.2. Steady Boundary Layer Problem*

Consider the advection-diffusion equation in $x \in (0, 1)$ with $u(0) = 0$ and $u(1) = 1$:

$$\partial_t u + a\partial_x u = \nu \partial_{xx} u + s(x), \tag{74}$$

where

$$s(x) = \frac{\pi}{Re}[a\cos(\pi x) + \pi\nu \sin(\pi x)], \;\; Re = a/\nu. \tag{75}$$

This is a boundary layer problem with a non-trivial steady state solution in the diffusion limit as a result of the source term addition [2]. This equation develops a very narrow boundary

Table 3: Spatial accuracy with the third-order RD-GT scheme for the steady linear advection-diffusion problem ($Re = 1$).

| Number of nodes | $L_1$ error of $u$ | Order | $L_1$ error of $p$ | Order |
|---|---|---|---|---|
| 10 | 9.54E-03 | | 8.59E-02 | |
| 25 | 4.63E-04 | 3.30 | 4.41E-03 | 3.24 |
| 50 | 4.85E-05 | 3.25 | 4.63E-04 | 3.25 |
| 100 | 5.46E-06 | 3.15 | 5.16E-05 | 3.17 |
| 200 | 6.46E-07 | 3.08 | 6.04E-06 | 3.09 |
| 300 | 1.88E-07 | 3.04 | 1.75E-06 | 3.05 |
| 500 | 3.99E-08 | 3.03 | 3.71E-07 | 3.04 |
| 1000 | 4.93E-09 | 3.02 | 4.57E-08 | 3.02 |

Table 4: Spatial accuracy with the fourth-order RD-D scheme for the steady linear advection-diffusion problem, $Re = 1$. (Note: fourth-order RD-D and RD-GT schemes produce almost identical result.)

| Number of nodes | $L_1$ error of $u$ | Order | $L_1$ error of $p$ | Order |
|---|---|---|---|---|
| 10 | 8.38E-03 | | 6.36E-02 | |
| 25 | 2.84E-04 | 3.69 | 1.82E-03 | 3.88 |
| 50 | 1.74E-05 | 4.03 | 1.02E-04 | 4.16 |
| 100 | 1.04E-06 | 4.07 | 5.77E-06 | 4.15 |
| 200 | 6.23E-08 | 4.06 | 3.35E-07 | 4.11 |
| 300 | 1.21E-08 | 4.04 | 6.44E-08 | 4.07 |
| 500 | 1.55E-09 | 4.02 | 8.15E-09 | 4.05 |
| 1000 | 9.30E-11 | 4.06 | 4.94E-10 | 4.04 |

Table 5: Spatial accuracy with the sixth-order RD-GT scheme for the steady linear advection-diffusion problem ($Re = 1$).

| Number of nodes | $L_1$ error of $u$ | Order | $L_1$ error of $p$ | Order |
|---|---|---|---|---|
| 10 | 2.60E-03 | | 1.75E-02 | |
| 25 | 3.34E-05 | 4.75 | 1.98E-04 | 4.89 |
| 50 | 4.87E-07 | 6.10 | 2.87E-06 | 6.11 |
| 100 | 4.32E-09 | 6.82 | 2.65E-08 | 6.76 |
| 200 | 3.09E-11 | 7.13 | 1.78E-10 | 7.22 |
| 300 | 5.80E-12 | – | 3.39E-11 | – |
| 500 | 3.60E-12 | – | 1.97E-11 | – |

layer near the right boundary ($x = 1$) when the advection term becomes dominant. The exact steady state solution to this problem is given by (see also Fig. 7).

$$u^{exact}(x) = \frac{e^{-Re} - e^{(x-1)Re}}{e^{-Re} - 1} + \frac{1}{Re}\sin(\pi x). \tag{76}$$

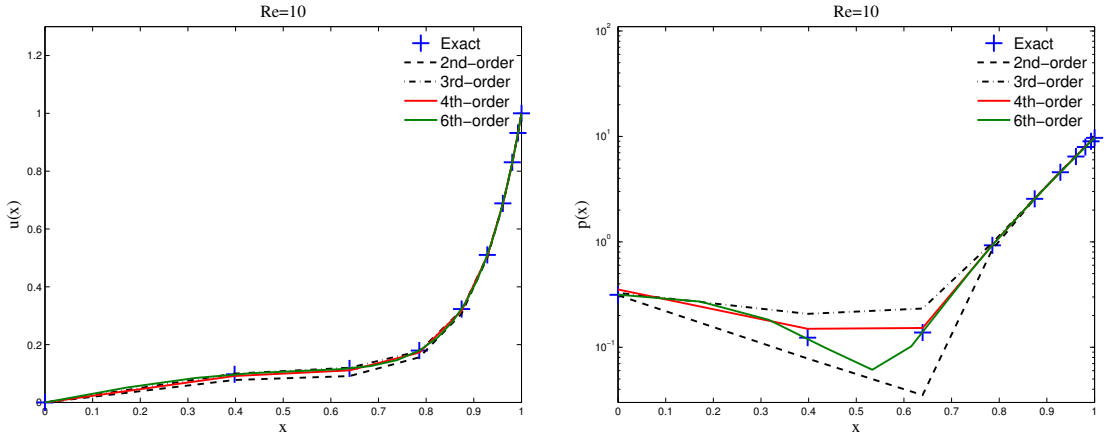


(a) $u(x)$ (b) $p(x) = du/dx$

Figure 7: Comparisons between the exact and the numerical results using the proposed high-order RD schemes for the steady boundary layer problem ($Re = 10$) on a nonuniform grid with $N = 10$.

We chose various $Re$ values ranging from 1 to $10^6$ and solved the equation on nonuniform grid sizes up to 100000 nodes. Like the previous problem, the solutions were obtained with the Newton-GS method. Within each Newton iteration, the GS relaxation were conducted until three orders of magnitude reduction is achieved for the linear system, and the residuals

of both the solution and the solution gradient were reduced by eight orders of magnitude. The convergence data are given in Table 6 for the proposed high-order RD schemes. The data are shown for the high-order schemes developed with the generalized trapezoidal rule. Similar results were obtained with the RD schemes developed with the divergence formulation, and therefore not shown. But in general, the high-order RD schemes with the generalized trapezoidal rule perform better than the ones developed with the divergence formulation. The latter third-order RD-D scheme not only produce slightly larger errors as shown in Fig. 6, but also encounter some convergence difficulties (particularly with time-dependent problems); the convergence problem seems originated from the lack of diagonal dominance caused by the particular structure of the source term discretization as shown in Section 4.1. We will therefore mainly focus on the RD-GT schemes for unsteady cases. The $O(N)$ linear dependency of the GS relaxations on the grid size is also demonstrated, which is a consequence of solving the advection-diffusion equation as a hyperbolic system. We emphasize that this is remarkable because the linear convergence is retained for any irregular grid in any dimensions ($N$ is approximately the number of nodes in each coordinate direction in two and three dimensions) as demonstrated in Refs. [1, 2, 3, 6, 4, 5]. It leads to orders of magnitude faster convergence in comparison with conventional methods whose convergence is typically $O(N^2)$ as discussed also in the previous paper [6]. Furthermore, the proposed high-order RD schemes are extremely efficient as the solutions were obtained with only a small number of Newton iterations: less than 10 iterations to reduce the residual by eight orders of magnitude. Moreover, the number of GS relaxations and Newton iterations are essentially independent of the scheme order. Considering the fact that the cost of one GS relaxation is significantly cheaper than one Newton iteration, we find that the developed high-order RD schemes are extremely powerful and efficient. Finally, as in the previous work [6], we remark that the high-$Re$ cases required extremely fine grids to meet the well-known requirement on the mesh Reynolds-number [2]. If desired, the computations can be performed on substantially coarser grids with more aggressive and customized grid stretching. However, we simply refined the grid to meet the mesh Reynolds-number requirement because our method is powerful enough to solve the problem very efficiently (i.e., less than 10 Newton iterations) even on such dense grids for all third-, fourth-, and sixth-order schemes. The ability to efficiently solve the problem on highly refined grids is a great advantage of these schemes.

Table 6: Steady boundary layer problem (Convergence criteria: Residuals $< 10^{-8}$.)

| $\log_{10} Re$ | Number of nodes | RD-GT Scheme Order | GS relaxations/Newton iteration | Newton iteratio |
|---|---|---|---|---|
| 0 | 50 | 3rd | 163 | 8 |
| | | 4th | 163 | 8 |
| | | 6th | | |
| 0 | 100 | 3rd | 324 | 7 |
| | | 4th | 324 | 7 |
| | | 6th | | |
| 0 | 500 | 3rd | 1647 | 7 |
| | | 4th | 1647 | 7 |
| | | 6th | | |
| 1 | 100 | 3rd | 178 | 7 |
| | | 4th | 178 | 7 |
| | | 6th | | |
| 2 | 100 | 3rd | 44 | 7 |
| | | 4th | 44 | 7 |
| | | 6th | | |
| 3 | 500 | 3rd | 42 | 8 |
| | | 4th | 43 | 7 |
| | | 6th | | |
| 4 | 1000 | 3rd | 18 | 9 |
| | | 4th | 19 | 7 |
| | | 6th | | |
| 5 | 10000 | 3rd | 24 | 9 |
| | | 4th | 21 | 7 |
| | | 6th | | |
| 6 | 100000 | 3rd | 18 | 9 |
| | | 4th | 19 | 7 |
| | | 6th | | |

The order of accuracy of the proposed RD schemes were also verified for this problem. Figures 8 shows the $L_1$ error convergence results, where $h$ is the representative mesh spacing defined by $h = /(N-1)$. For discussion purposes, we present the accuracy plots for $Re = 1$ and $Re = 10$; similar results were obtained for other Reynolds numbers. These results verify the order of accuracy of the proposed high-order RD schemes (i.e., third-, fourth-, and sixth-order) for all the variables and the gradients at all the grid nodes including the boundary nodes (see also Tables 7, 8, and 9). Note that when the differences between the numerical results and exact values approach the machine zero, the $L_1$ slope approaches zeroth-order; these data are omitted from the Tables 8 and 9.

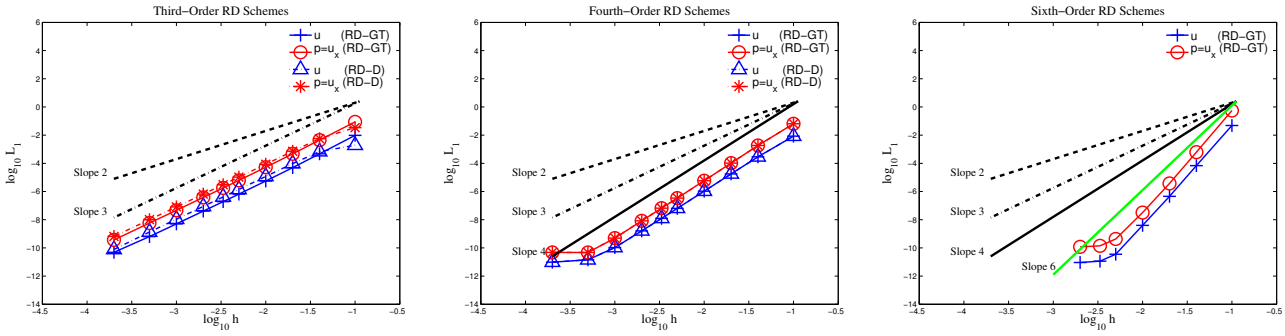


(a) third-order ($Re = 1$) (b) fourth-order ($Re = 1$) (c) sixth-order ($Re = 10$)

Figure 8: $L_1$ error of the proposed high-order RD hyperbolic schemes for the boundary layer problem on nonuniform grids.

### *6.3. Unsteady Linear Advection-Diffusion*

Consider the time-dependent advection-diffusion equation in $x \in (0, 1)$

$$\partial_t u + a\partial_x u = \nu \partial_{xx} u. \tag{77}$$

The above equation with the following initial condition:

$$u(x, t = 0) = \sin(\kappa x), \tag{78}$$

where $\kappa$ is an arbitrary constant, has the following exact solution with a periodic boundary condition:

$$u^{exact}(x, t) = e^{-\kappa^2 \nu t} \sin(\kappa(x - at)). \tag{79}$$

A non-periodic solution also exists for the following oscillatory boundary conditions

$$u(0, t) = 0, \tag{80}$$

$$u(1, t) = U \cos(\omega t), \tag{81}$$

Table 7: Spatial accuracy with the third-order RD-GT scheme for the boundary layer problem with $Re = 1.0$.

| Number of nodes | $L_1$ error of $u$ | Order | $L_1$ error of $p$ | Order |
|---|---|---|---|---|
| 10 | 9.65E-03 | | 8.68E-02 | |
| 25 | 4.70E-04 | 3.30 | 4.47E-03 | 3.24 |
| 50 | 4.94E-05 | 3.25 | 4.70E-04 | 3.25 |
| 100 | 5.56E-06 | 3.15 | 5.26E-05 | 3.16 |
| 200 | 6.58E-07 | 3.08 | 6.16E-06 | 3.09 |
| 300 | 1.91E-07 | 3.06 | 1.79E-06 | 3.05 |
| 500 | 4.07E-08 | 3.03 | 3.79E-07 | 3.04 |
| 1000 | 5.04E-09 | 3.01 | 4.66E-08 | 3.02 |
| 2000 | 6.34E-10 | 2.99 | 5.79E-09 | 3.01 |
| 5000 | 4.89E-11 | 2.80 | 3.68E-10 | 3.00 |

Table 8: Spatial accuracy with the fourth-order RD-GT schemes for the boundary layer problem with $Re = 1.0$. Note that when the differences between the numerical results and exact values approach the machine zero, the $L_1$ slope approaches zeroth-order.

| Number of nodes | $L_1$ error of $u$ | Order | $L_1$ error of $p$ | Order |
|---|---|---|---|---|
| 10 | 8.48E-03 | | 6.43E-02 | |
| 25 | 2.88E-04 | 3.69 | 1.84E-03 | 3.88 |
| 50 | 1.78E-05 | 4.02 | 1.04E-04 | 4.14 |
| 100 | 1.06E-06 | 4.07 | 5.87E-06 | 4.15 |
| 200 | 6.41E-08 | 4.05 | 3.42E-07 | 4.10 |
| 300 | 1.25E-08 | 4.04 | 6.57E-08 | 4.07 |
| 500 | 1.61E-09 | 4.01 | 4.35E-09 | 4.05 |
| 1000 | 1.06E-10 | 3.92 | 4.98E-10 | 4.06 |
| 2000 | 1.42E-11 | – | 1.42E-11 | – |
| 5000 | 9.69E-12 | – | 4.75E-11 | – |

Table 9: Spatial accuracy with the sixth-order RD-GT scheme for the boundary layer problem with $Re = 10$.

| Number of nodes | $L_1$ error of $u$ | Order | $L_1$ error of $p$ | Order |
|---|---|---|---|---|
| 10 | 4.81E-02 | | 5.54E-01 | |
| 25 | 6.89E-05 | 4.75 | 6.19E-04 | 4.89 |
| 50 | 4.54E-07 | 6.11 | 3.76E-06 | 6.11 |
| 100 | 3.97E-09 | 6.78 | 3.21E-08 | 6.73 |
| 200 | 3.56E-11 | 7.59 | 4.28E-10 | 7.37 |
| 300 | 1.14E-11 | – | 1.40E-10 | – |
| 500 | 9.23E-12 | – | 1.19E-10 | – |

where $U$ is the amplitude of the oscillation and $\omega$ is the frequency of the oscillation on the right boundary. The exact solution is given by

$$u^{exact}(x,t) = Real\left(\frac{e^{\lambda_1 x} - e^{\lambda_2 x}}{e^{\lambda_1} - e^{\lambda_2}} U e^{i\omega t}\right), \ \lambda_{1,2} = \frac{a \pm \sqrt{a^2 + 4i\omega\nu}}{2\nu}, \tag{82}$$

where $i = \sqrt{-1}$.

We solved the above two problems with the first-order hyperbolic advection-diffusions equation given as in Eq. (2) and (3). For each physical time, we reduced the residuals by two orders of magnitude before advancing in time. During each time step, we also relaxed the linear system using GS relaxations until two orders of magnitude reduction in the linear system residuals was achieved (see Figs. 9 and 10.) We also note that more residual reduction in pseudo time may be necessary on more complex problems but two orders of magnitude reduction in the residuals were sufficient for the problems presented here.

We examined the convergence rate of these problems on several uniform and nonuniform grid systems. Given in Tables 10 and 11 are the average numbers of GS relaxations per Newton iteration obtained over 100 time steps for the periodic and the oscillatory boundary condition problems, respectively. Clearly the convergence rate of the GS relaxation is of $O(N)$, not $O(N^2)$ as typical for numerical methods for the advection-diffusion equation. Observe that for most grid systems only two Newton iterations were sufficient to obtain accurate solutions regardless of the scheme order. We also note that we used $\Delta t = 0.01$ for all the grid systems. The maximum grid spacing used is about 0.04. The corresponding CFL value is then about 6.5 (based on $\Delta t = 0.01$), which is significantly smaller that the maximum-allowable CFL values obtained with the Fourier analysis for all the BDF

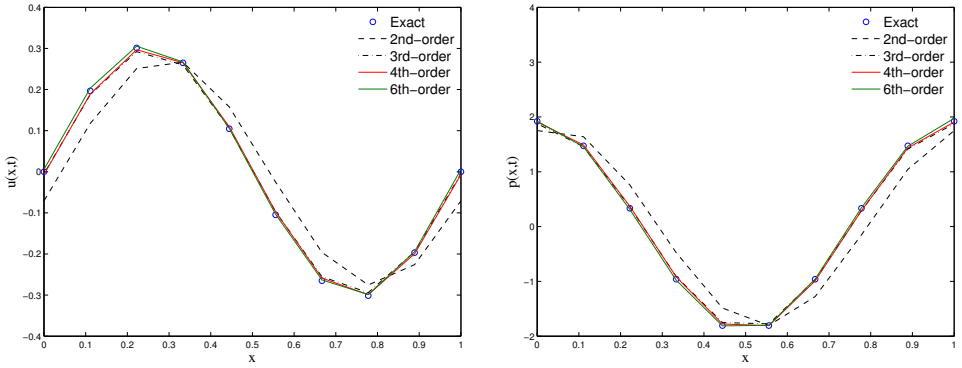


(a) $u(x, t = 1.0)$ (b) $p(x, t = 1.0) = du/dx$

Figure 9: Time-dependent linear advection-diffusion problem ($Re = 33.33$) with periodic boundary condition on $N = 10$ uniform nodes ($\Delta t = 0.01$.)

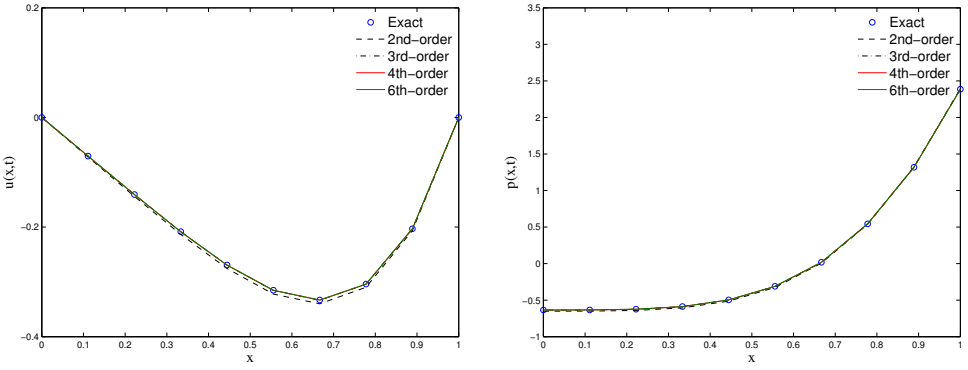


(a) $u(x, t = 1.0)$ (b) $p(x, t = 1.0) = du/dx$

Figure 10: Time-dependent linear advection-diffusion problem with oscillatory boundary condition ($\omega = 7\pi/2$, $\kappa = 2\pi$, $U = 1$, $\nu = 1$) on $N = 10$ uniform nodes ($\Delta t = 0.01$.)

methods (see Appendix A). Note that the maximum-allowable CFL value increases with grid refinement. The time step is orders-of-magnitude larger than that required for

Table 10: Unsteady linear advection-diffusion problem with periodic BC ($a = 1, \nu = 0.03$) on uniform grids. Average data over 100 time steps are given. (Convergence criteria: Residuals $< 10^{-2}$)

| Number of nodes | RD-GT Scheme Order | GS relaxations/Newton iteration | Newton iteration |
|---|---|---|---|
| 25 | 3rd | 5 | 4 |
| | 4th | 5 | 4 |
| | 6th | 6 | 5 |
| 100 | 3rd | 24 | 2 |
| | 4th | 24 | 2 |
| | 6th | 24 | 2 |
| 300 | 3rd | 33 | 2 |
| | 4th | 35 | 2 |
| | 6th | 35 | 2 |
| 500 | 3rd | 55 | 2 |
| | 4th | 55 | 2 |
| | 6th | 55 | 2 |
| 1000 | 3rd | 116 | 2 |
| | 4th | 116 | 2 |
| | 6th | 116 | 2 |

conventional explicit schemes, which is limited by $O(h^2)$. Of course, conventional implicit schemes also allow unconditionally large time steps, but it requires $O(N^2)$ convergence in an iterative linear solver and potentially a much larger number of outer iterations as well if the exact linearization is not possible and Newton's method cannot be constructed. Hence, the method developed here has two major advantages over conventional methods: the second order Jacobian formulation and $O(N)$ iterative convergence in the linear solver. The latter advantage can be potentially huge with increase of the grid system as the speed-up factor is $O(N)$ and thus grows for finer grids. Note also that the second-order Jacobian formulation is the advantage of the RD scheme over finite volume schemes where the compact Jacobian formulation is only first-order. The results also show that the convergence rate is the same

Table 11: Unsteady linear advection-diffusion problem with oscillatory BC ($\omega = 7\pi/2, a = 1.$) on nonuniform grids. Average data over 100 time steps are given. (Convergence criteria: Residuals $< 10^{-2}$)

| Number of nodes | RD-GT Scheme Order | GS relaxations/Newton iteration | Newton iteration |
|---|---|---|---|
| 25 | 3rd | 35 | 4 |
| | 4th | 37 | 4 |
| | 6th | 45 | 4 |
| 50 | 3rd | 69 | 4 |
| | 4th | 72 | 4 |
| | 6th | 72 | 4 |
| 100 | 3rd | 136 | 4 |
| | 4th | 142 | 4 |
| | 6th | 142 | 4 |
| 500 | 3rd | 650 | 4 |
| | 4th | 680 | 4 |
| | 6th | 680 | 4 |
| 1000 | 3rd | 1283 | 4 |
| | 4th | 1332 | 4 |
| | 6th | 1332 | 4 |

for all the developed high-order RD schemes. It means that the only cost to these higher order schemes is the evaluation of the first and the second derivatives of the source terms and in the case of the fourth-order scheme with the generalized trapezoidal rule, the second derivatives are not required.

We verified the order of accuracy of the proposed schemes on time-dependent linear problems with consistent space-time discretization; i.e., third-order with BDF3, fourth-order with BDF4, and sixth-order with BDF6. The same spatial order of accuracy can be observed with the *A-Stable* BDF2 with small enough time steps such that the temporal error is comparable to the spatial error (i.e., $\Delta t^2 \sim h^m$, where $m$ is the scheme order). But the consistent pair of BDF and spatial discretization allows about two orders of magnitude reduction in the number of time steps for the finest grid cases. Note that time-accurate computations are started by BDF1 in the first time step with extremely small time step (e.g. $\Delta t = 10^{-8}$), and then by higher order BDFs thereafter with much larger time steps (e.g. $\Delta t = 0.01$). This will ensure the order of accuracy of the developed higher order schemes through all times. We remark that explicit time stepping is not available for time-accurate computations with the hyperbolic system method (see Ref. [6] for more details.)

Figure 11 shows the $L_1$ error convergence for the above time-dependent linear problem with the oscillatory boundary condition (see also Tables 12, 13, and 14), where clearly the order of accuracy of the proposed schemes are verified for the linear time-dependent problems. The results were obtained at $t = 1.0$. We used the same $\Delta t$ among the third-, fourth- and sixth-order schemes and were able to obtain the desired order of accuracy. (Note that we showed the RD schemes that were developed with the generalized trapezoidal rule as these are more efficient and less expensive than the ones developed with divergence formulation of the source terms.)

### *6.4. Unsteady Nonlinear Advection-Diffusion*

Consider the unsteady nonlinear viscous Burgers equation with an unsteady time-dependent source term:

$$\partial_t u + \partial_x f = \partial_x \left(\nu \, u_x\right) + S(x,t), \quad x \in (0,1), \tag{83}$$

where $f = u^2/2$, $\nu = u$, and

$$S(x,t) = \partial_t u^e + \frac{1}{2}\partial_x (u^e)^2 - \partial_x (u^e p^e), \tag{84}$$

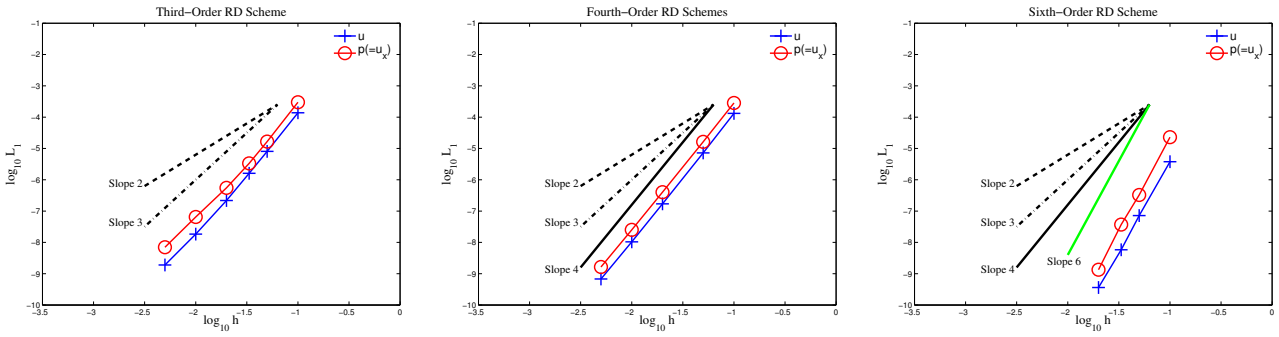


(a) third-order + BDF3 (b) fourth-order + BDF4 (c) sixth-order + BDF6

Figure 11: Spatial accuracy of the proposed high-order RD-GT hyperbolic schemes for the time-dependent linear problem with oscillatory BC on uniform grids.

Table 12: Spatial accuracy for the linear time dependent problem with oscillatory BC ($\omega = 7\pi/2, a = 1.$) using the third-order RD-GT scheme with the BDF3 time discretization.

| Number of nodes | $\Delta t$ (BDF3) | $L_1$ error of $u$ | Order | $L_1$ error of $p$ | Order |
|---|---|---|---|---|---|
| 10 | 2.50E-03 | 1.40E-04 | | 2.86E-04 | |
| 20 | 2.50E-03 | 9.06E-06 | 3.95 | 1.90E-05 | 3.91 |
| 50 | 1.25E-03 | 3.54E-07 | 3.54 | 7.38E-07 | 3.54 |
| 100 | 5.00E-04 | 2.57E-08 | 3.78 | 4.71E-08 | 3.97 |
| 200 | 2.50E-04 | 2.59E-09 | 3.31 | 4.40E-09 | 3.42 |

Table 13: Spatial accuracy for the linear time dependent problem with oscillatory BC ($\omega = 7\pi/2, a = 1.$) using the fourth-order RD-GT scheme with the BDF4 time discretization.

| Number of nodes | $\Delta t$ (BDF4) | $L_1$ error of $u$ | Order | $L_1$ error of $p$ | Order |
|---|---|---|---|---|---|
| 10 | 2.50E-03 | 1.32E-04 | | 2.83E-04 | |
| 20 | 2.50E-03 | 7.22E-06 | 4.19 | 1.63E-05 | 4.12 |
| 50 | 1.25E-03 | 1.70E-07 | 4.09 | 4.01E-07 | 4.04 |
| 100 | 5.00E-04 | 1.04E-08 | 4.03 | 2.51E-08 | 4.00 |
| 200 | 2.50E-04 | 6.78E-10 | 3.94 | 1.64E-09 | 3.94 |

Table 14: Spatial accuracy for the linear time dependent problem with oscillatory BC ($\omega = 7\pi/2, a = 1.$) using the sixth-order RD-GT scheme with the BDF6 time discretization.

| Number of nodes | $\Delta t$ (BDF6) | $L_1$ error of $u$ | Order | $L_1$ error of $p$ | Order |
|---|---|---|---|---|---|
| 10 | 2.50E-03 | 3.77E-06 | | 2.29E-05 | |
| 20 | 2.50E-03 | 7.19E-08 | 5.71 | 3.27E-07 | 6.13 |
| 50 | 1.25E-03 | 5.81E-09 | 6.20 | 3.70E-08 | 5.37 |
| 100 | 5.00E-04 | 3.62E-10 | 5.43 | 1.34E-09 | 6.50 |

where $p^e = \partial_x u^e$. The source term has been generated by the following function:

$$u^e(x,t) = Real\left(\frac{\sinh(x\sqrt{i\omega/\nu})}{\sinh(\sqrt{i\omega/\nu})} U e^{i\omega t}\right) + C,\ C > 1, \tag{85}$$

so that it is the exact solution to Eq. (83) with the boundary conditions defined as

$$u(0,t) = C, \tag{86}$$

$$u(1,t) = C + U\cos(\omega t), \tag{87}$$

where $\omega$ is the frequency of the oscillation on the right boundary, and $U$ is the amplitude of the oscillation. We note that the constant $C$ must be greater than 1 in order for the diffusion coefficient to be positive. We solved this time-dependent nonlinear advection-diffusion equation with the following equivalent first-order hyperbolic system (see Ref. [6] for more details):

$$\partial_\tau u + \partial_x\left(u^2\right) = \partial_x p - \partial_t u + S(x,t), \tag{88}$$

$$\frac{T_r}{\nu}\partial_\tau p = (\partial_x u - p/\nu). \tag{89}$$

For this nonlinear unsteady problem, the manufactured source term contains terms that are already in the divergence form; i.e. the residual evaluation of these terms are exact. The $\partial_t u^e$ term is the only term in the manufactured source term with a non-exact residual evaluation. The BDF discretization of the $\partial_t u$ term in Eq. (88) will not be in the divergence form and therefore will not have an exact residual evaluation. In addition, the second equation has a nonlinear source term, $p/\nu$ (note that here $\nu = u$). We obtained the high-order results by evaluating all of these non-exact residuals using the proposed techniques. Newton iterations are taken to be converged when the overall residuals are dropped by eight orders

of magnitude. For each Newton iteration, we relaxed the linear system until the residuals are reduced by two orders of magnitude.

The $O(N)$ convergence rate of the GS relaxations was once again achieved for the time-dependent nonlinear hyperbolic advection-diffusion system. This is given in Table 15, where the average number of iterations were obtained over 1000 time steps (over 17 periods). Note also that the high-order RD schemes converged with only ten Newton iterations with the compact second-order Jacobian formulation. It is remarkable that such a rapid convergence is achieved for all high-order schemes with the second-order Jacobian.

Table 15: Unsteady nonlinear advection-diffusion problem ($\nu = a = u$) with oscillatory BC ($U = 1$, $C = 2$, $\omega = 7\pi/2$) on nonuniform grids. Average data over 1000 time steps are given. (Convergence criteria: GS Relaxation $< 10^{-2}$; Newton residuals $< 10^{-8}$).

| Number of nodes | RD-GT Scheme Order | GS relaxations/Newton iteration | Newton iteration |
|---|---|---|---|
| 50 | 3rd | 435 | 10 |
| | 4th | 430 | 10 |
| | 6th | 431 | 10 |
| 100 | 3rd | 879 | 10 |
| | 4th | 868 | 10 |
| | 6th | 864 | 10 |
| 200 | 3rd | 1772 | 10 |
| | 4th | 1749 | 10 |
| | 6th | 1737 | 10 |

Shown in Fig. 12 are the order of accuracy plots obtained for this unsteady advection-diffusion problem on series of nonuniform grids (see also Tables 16, 17, and 18). The results confirm the high-order accuracy of developed RD schemes for unsteady nonlinear problems on nonuniform grids. We also observe that our proposed sixth-order RD scheme, as discussed in the previous section, have in fact produced seventh-order accurate results demonstrating its power characteristics in efficiently providing very high accurate solutions and gradients (see Table 18 for more details). We note, however, that the seventh-order accuracy is not a general feature of the sixth-order scheme. Although it is not clear from the exact solution, it could be due to the sixth-order derivative of the source term in the leading truncation error being vanishingly small. We also note that the CFL, corresponding to the largest grid

spacing of about 0.04 used in this study, is about 30 for the $\Delta t = 0.00125$. This value is still within the range of the stability of all the BDF methods (see Appendix A for more details.) Note again that the maximum-allowable CFL increases with grid refinement.

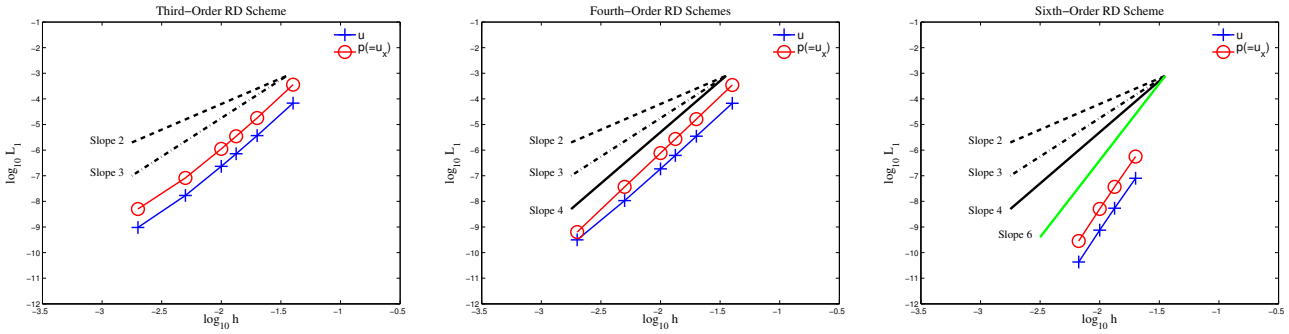


(a) third-order + BDF3 (b) fourth-order + BDF4 (c) sixth-order + BDF6

Figure 12: Spatial accuracy of the proposed high-order RD-GT hyperbolic schemes for the time-dependent nonlinear problem ($\nu = a = u$) with oscillatory BC ($U = 1$, $C = 2$, $\omega = 7\pi/2$) on nonuniform grids.

Table 16: Spatial accuracy for the time-dependent nonlinear problem ($\nu = a = u$) with oscillatory BC ($U = 1$, $C = 2$, $\omega = 7\pi/2$) using the third-order RD-GT scheme and BDF3 time discretization on nonuniform grids.

| Number of nodes | $\Delta t$ (BDF3) | $L_1$ error of $u$ | Order | $L_1$ error of $p$ | Order |
|---|---|---|---|---|---|
| 25 | 1.25E-03 | 6.83E-05 | | 3.59E-04 | |
| 50 | 1.25E-03 | 3.68E-06 | 4.21 | 1.79E-05 | 4.33 |
| 100 | 1.00E-03 | 2.33E-07 | 3.98 | 1.12E-06 | 4.00 |
| 200 | 5.00E-04 | 1.70E-08 | 3.78 | 8.23E-08 | 3.77 |
| 500 | 2.50E-04 | 9.58E-10 | 3.14 | 5.03E-09 | 3.05 |

## 7. Conclusions

In this paper, we have developed a series of efficient high-order Residual-Distribution (RD) schemes for general advection-diffusion problems. Third- and fourth-order RD schemes were developed with the divergence formulation of the source term. These schemes are very economical as they require only the evaluation of the first and second derivatives of the source term, and not of the solution. The first and second derivatives need to be second and first order accurate, respectively, on arbitrary grids, and they are obtained by a compact quadratic fit. Third-, fourth-, and sixth-order RD schemes are also developed with a

Table 17: Spatial accuracy for the time-dependent nonlinear problem ($\nu = a = u$) with oscillatory BC ($U = 1$, $C = 2$, $\omega = 7\pi/2$) using the fourth-order RD schemes and BDF4 time discretization on nonuniform grids.

| Number of nodes | $\Delta t$ (BDF4) | $L_1$ error of $u$ | Order | $L_1$ error of $p$ | Order |
|---|---|---|---|---|---|
| 25 | 1.25E-03 | 6.75E-05 | | 3.49E-04 | |
| 50 | 1.25E-03 | 6.21E-07 | 4.27 | 2.71E-06 | 4.23 |
| 100 | 1.00E-03 | 1.85E-07 | 4.24 | 7.68E-07 | 4.40 |
| 200 | 1.00E-03 | 1.07E-08 | 4.11 | 3.69E-08 | 4.38 |
| 500 | 5.00E-04 | 3.14E-10 | 3.85 | 6.33E-10 | 4.44 |

Table 18: Spatial accuracy for the time-dependent nonlinear problem ($\nu = a = u$) with oscillatory BC ($U = 1$, $C = 2$, $\omega = 7\pi/2$) using the sixth-order RD-GT scheme and BDF6 time discretization on nonuniform grids.

| Number of nodes | $\Delta t$ (BDF6) | $L_1$ error of $u$ | Order | $L_1$ error of $p$ | Order |
|---|---|---|---|---|---|
| 50 | 1.25E-03 | 7.99E-08 | | 5.61E-08 | |
| 75 | 5.00E-04 | 5.42E-09 | 6.60 | 3.69E-09 | 6.71 |
| 100 | 5.00E-04 | 7.54E-10 | 6.85 | 5.09E-09 | 6.91 |
| 200 | 5.00E-04 | 4.30E-11 | 7.06 | 2.83E-09 | 7.11 |

generalized trapezoidal rule. The third-order schemes require the evaluation of the first and second derivatives of the source term, which must be second and first order accurate, respectively. On the other hand, the fourth-order scheme requires only the second-order accurate gradients, and therefore is the least expensive scheme among all the developed high-order schemes in this paper. All third- and fourth-order schemes are constructed within a five-point stencil in the interior, a four-point stencil at the nodes adjacent to the boundary, and a three-point stencil at the boundary nodes. For the sixth-order scheme, the evaluation of the first and second derivatives of the source term is required, and they must be third- and second-order accurate, which is achieved by a cubic fit. It results in the stencil extension by one or two nodes in the nodal residual. In addition, the analysis of the proposed sixth-order RD scheme as well as the results presented here show that this high-order RD scheme can, in some cases, produce seventh-order results on nonuniform grids. An implicit steady solver is constructed based on the Jacobian derived from the compact second-order RD scheme. It is demonstrated that the solver achieves a rapid convergence like Newton's method for all high-order schemes despite the fact that the Jacobian is not exact. Specifically, it requires only a small number of Newton iterations, typically less than 10, for both steady and unsteady problems, even for highly refined grids, up to 100000 nodes. We have demonstrated also that all of these high-order schemes are capable of producing both high-order accurate solution and gradient on nonuniform grids very efficiently by less than ten Newton iterations.

The study presented in this paper should be of interest to researchers working on finite-volume schemes because the RD scheme is known to be equivalent to the finite-volume scheme in one dimension (see for example Ref. [24]). Specifically, a second-order upwind RD scheme is equivalent to the first-order finite-volume scheme with a special form of source term discretization [2]. It implies that the developed high-order RD schemes may also be implemented in the form of first-order finite-volume schemes with special source term discretization formulas. The resulting finite-volume schemes will be different from many other finite-volume schemes in that they do not require computations of solution gradients.

The developed high-order schemes could well bring significant improvements to the numerical methods for practical problems such as material thermal response calculations of thermal protection systems of atmospheric entry vehicles [17, 18, 19], and the experimental aeroheating data reduction [20, 21], which are based on one-dimensional analyses and routinely used in industries (e.g. NASA). A particularly useful scheme would be the fourth-

order scheme based on the generalized trapezoidal rule (RD-GT) because it requires only the second-order accurate gradients of the source term. Application to these practical problems should be undertaken and is left as future work.

Extensions to higher dimensions are highly desired. To extend the developed high-order schemes to higher dimensions, it is necessary to employ a high-order quadrature formula for integrating the flux divergence term, which has been integrated exactly in one dimension but cannot be integrated exactly in higher dimensions. For the source term discretization, the divergence formulation can be extended relatively straightforwardly while a discretization formula such as the generalized trapezoidal rule remains to be found. In particular, a third-order version is expected to be practical in multi-dimensions: a high-order quadrature formula with added edge-midpoints along with a quadratic fit for first-derivatives. The solution at the midpoint can be obtained by the Hermite interpolation along each edge, and thus does not need to be stored [12]. As a result, the number of degrees of freedom remains the same as the second-order scheme. It is expected to be a very efficient scheme compared with other high-order methods such as Discontinuous Galerkin or Spectral Volume methods.

Finally, extensions to more complex nonlinear equations such as the Navier-Stokes equations remain as a challenge. For the compressible Navier-Stokes equations, the complete eigen-structure of the whole system has yet to be found. The construction of the upwind RD scheme based on a single hyperbolic system, as presented in this paper, is a challenge. To overcome the difficulty, a simplified approach has been proposed and demonstrated for a finite-volume scheme in Ref. [3], which is based on the independent treatment of the inviscid and viscous terms. A similar approach may become necessary for the RD schemes.

**Acknowledgments**

The second author is supported by the U.S. Army Research Office under the contract/grant number W911NF-12-1-0154.

## Appendix A. BDF Stability Analysis on the Proposed High Order RD Schemes

Consider a Fourier mode of non dimensional wave number $\beta \in [0, \pi]$ on a uniform mesh of spacing $h$:

$$\mathbf{U}^{\beta} = \mathbf{U}_0(t) e^{i\beta(x-x_j)/h}, \tag{A.1}$$

where $\mathbf{U}^\beta = (u^\beta, p^\beta)$ and $\mathbf{U}_0(t) = (u_0(t), p_0(t))$. Applying this Fourier mode to the discretized first order hyperbolic system, we arrive at:

$$\mathbf{N}^\beta \frac{d\mathbf{U}_0}{dt} = \mathbf{M}^\beta \mathbf{U}_0, \tag{A.2}$$

where $\mathbf{M}^\beta$ and $\mathbf{N}^\beta$ are, respectively, the spatial operators for the spatial and temporal terms of the system. Note that the spatial operator arises from the temporal term because the physical time derivative is discretized in space and distributed to the nodes in our schemes. The matrix $\mathbf{N}^\beta$ may be called the mass matrix.

The spatial operator $\mathbf{M}^\beta$ is defined as:

$$\mathbf{M}^\beta = \frac{1}{h}(\mathbf{B}^+ \mathbf{J}_{\mathbf{\Phi}^L} + \mathbf{B}^- \mathbf{J}_{\mathbf{\Phi}^R}), \tag{A.3}$$

where

$$\mathbf{J}_{\mathbf{\Phi}^L} = \begin{bmatrix} -a(e^{i\beta}-1) & \nu(e^{i\beta}-1) \\ (e^{i\beta}-1)/T_r & S^\beta_{\mathbf{\Phi}^L} \end{bmatrix}, \quad \mathbf{J}_{\mathbf{\Phi}^R} = \begin{bmatrix} -a(1-e^{-i\beta}) & \nu(1-e^{-i\beta}) \\ (1-e^{-i\beta})/T_r & S^\beta_{\mathbf{\Phi}^R} \end{bmatrix}. \tag{A.4}$$

The $S^\beta$ is associated with the source term and therefore depends on the proposed source term discretization. For discussion purposes, here we only consider high order RD-GT schemes and the corresponding source terms become:

$$S^\beta_{\mathbf{\Phi}^R} = \frac{h}{2T_r} \begin{cases} e^{i\beta} + 1 + A^R + B^R : \text{3rd-order} \\ e^{i\beta} + 1 + A^R : \text{4th-order} \\ e^{i\beta} + 1 + C^R + D^R : \text{6th-order} \end{cases} \tag{A.5}$$

$$S^\beta_{\mathbf{\Phi}^L} = \frac{h}{2T_r} \begin{cases} e^{-i\beta} + 1 + A^L + B^L : \text{3rd-order} \\ e^{-i\beta} + 1 + A^L : \text{4th-order} \\ e^{-i\beta} + 1 + C^L + D^L : \text{6th-order} \end{cases} \tag{A.6}$$

where,

$$A^R = (e^{i\beta} - e^{-i\beta} - e^{2i\beta} + 1)/12 \tag{A.7}$$

$$B^R = (-e^{i\beta} + e^{-i\beta} - e^{2i\beta} - 3)/1000 \tag{A.8}$$

$$C^R = (-e^{-2i\beta} + 3e^{-i\beta} - 2e^{i\beta} + 3e^{2i\beta} - e^{3i\beta} - 2)/12 \tag{A.9}$$

$$D^R = (-e^{i\beta} + e^{-i\beta} + e^{2i\beta} - 1)/60 \tag{A.10}$$

$$A^L = (-e^{i\beta} + e^{-i\beta} - e^{-2i\beta} - 1)/10 \tag{A.11}$$

$$B^L = (-e^{i\beta} - 3e^{-i\beta} + e^{-2i\beta} - 3)/1000 \tag{A.12}$$

$$C^L = (4e^{-2i\beta} - 2e^{-i\beta} + 3e^{i\beta} - e^{2i\beta} - e^{-3i\beta} - 2)/12 \tag{A.13}$$

$$D^L = (e^{i\beta} - e^{-i\beta} + e^{-2i\beta} + 1)/60 \tag{A.14}$$

The mass matrix $\mathbf{N}^\beta$ is defined as:

$$\mathbf{N}^\beta = \frac{1}{h}(\mathbf{B}^+\mathbf{J}^t_{\mathbf{\Phi}^L} + \mathbf{B}^-\mathbf{J}^t_{\mathbf{\Phi}^R}), \tag{A.15}$$

where

$$\mathbf{J}^t_{\mathbf{\Phi}^L} = T_r \begin{bmatrix} S^\beta_{\mathbf{\Phi^L}} & 0 \\ 0 & 0 \end{bmatrix}, \quad \mathbf{J}^t_{\mathbf{\Phi}^R} = T_r \begin{bmatrix} S^\beta_{\mathbf{\Phi^R}} & 0 \\ 0 & 0 \end{bmatrix}. \tag{A.16}$$

Note that only the variable $u$ evolves with the BDF. Thus, we can eliminate the $p_0$ by solving the second equation in the system (A.2) and substituting it back to the first equation and arrive at:

$$\mathrm{BDF}(u_0) = \lambda^\beta u_0, \tag{A.17}$$

where $\mathrm{BDF}(u_0)$ denotes the time discretization of $du_0/dt$ by the BDF, and

$$\lambda^\beta = \frac{M^\beta_{(1,1)} - M^\beta_{(1,2)}M^\beta_{(2,1)}/M^\beta_{(2,2)}}{N^\beta_{(1,1)} - M^\beta_{(1,2)}N^\beta_{(2,1)}/M^\beta_{(2,2)}}. \tag{A.18}$$

With the physical time step defined as $\Delta t = \mathrm{CFL}\, h/(a + \nu/h)$, the quantity relevant to the stability $\lambda^\beta \Delta t$ can be shown to depend only on two parameters: $ReL_r = aL_r/\nu$ and the mesh-Reynolds-number $Reh = ah/\nu$. The former is essentially equivalent to the global Reynolds number, $Re = a/\nu$ since $Lr = O(1)$ (see [6] for details); it plays a role of properly weighting the upwind advection and the upwind diffusion schemes [2].

We now numerically perform stability analysis for BDF3, BDF4, and BDF6 and estimate the maximum-allowable CFL ($= \Delta t\,(a+\nu/h)/h$) values for different mesh sizes and $Re = a/\nu$ numbers. Shown in Fig. A.13 are the stability regions and maximum CFL values graphically illustrated corresponding to the proposed time-dependent high-order RD-GT schemes. Table A.19 provides maximum CFL for ranges of $Re$ and grid spacing for the high order schemes. Observe that the maximum-allowable CFL number varies significantly with $Re$ on a given mesh, but it is essentially the same for the same $Reh$. Note that $Reh < 2$ is required to avoid numerical oscillations [2], and the maximum-allowable CFL number in this range is large enough to perform practical computations.

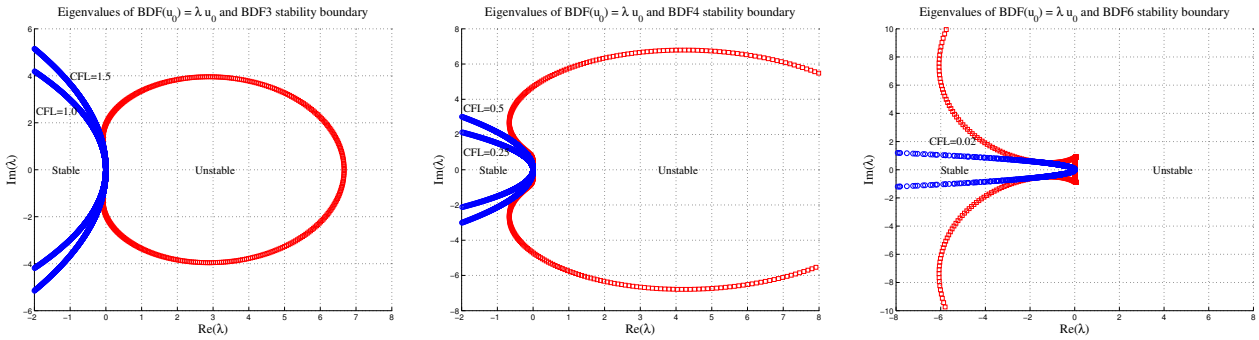


(a) BDF3 with 3rd-order RD-GT (b) BDF4 with 4th-order RD-GT (c) BDF6 with 6th-order RD-GT

Figure A.13: Maximum-allowable CFL for the proposed high-order time-dependent RD schemes ($h = 0.1$, $Re = 100$). The stable region is bounded by a curve represented by the red circles. The eigenvalues of the discretizaiton are plotted in blue and all contained in the stable region for the maximum CFL number.

Table A.19: Maximum-allowable CFL values for the proposed high-order unsteady RD hyperbolic advection-diffusion schemes.

| | $Re = 1$ | | | $Re = 100$ | | | $Re = 10^6$ | | |
|---|---|---|---|---|---|---|---|---|---|
| Grid spacing | BDF3 | BDF4 | BDF6 | BDF3 | BDF4 | BDF6 | BDF3 | BDF4 | BDF6 |
| 0.1 | 1000 | 500 | 20 | 1.5 | 0.5 | 0.02 | | | |
| 0.01 | 90000 | 50000 | 1800 | 25 | 10 | 0.35 | | | |
| 0.001 | | | | 1500 | 500 | 20 | 0.04 | 0.005 | 0.0002 |
| 0.0001 | | | | 150000 | 50000 | 2000 | 0.15 | 0.05 | 0.002 |
| 0.00001 | | | | | | | 1.5 | 0.5 | 0.02 |
| 0.000001 | | | | | | | 25 | 10 | 0.3 |

## References


[1] H. Nishikawa. A first-order system approach for diffusion equation. I: Second-order residual-distribution schemes. *J. Comput. Phys.*, 227:315–352, 2007.

[2] H. Nishikawa. A first-order system approach for diffusion equation. II: Unification of advection and diffusion. *J. Comput. Phys.*, 229:3989–4016, 2010.

[3] H. Nishikawa. New-generation hyperbolic Navier-Stokes schemes: $O(1/h)$ speed-up and accurate viscous/heat fluxes. In *20th AIAA Computational Fluid Dynamics Conference*, AIAA Paper 2011-3043, Hawaii, 2011.

[4] H. Nishikawa. First-, second-, and third-order finite-volume schemes for diffusion. *J. Comput. Phys.*, 256:791–805, 2014.

[5] H. Nishikawa. First, second, and third order finite-volume schemes for advection-diffusion. *J. Comput. Phys.*, 2014. accepted.

[6] A. Mazaheri and H. Nishikawa. First-order hyperbolic system method for time-dependent advection-diffusion problems. *NASA/TM-2014-218175*, 2014.

[7] H. Deconinck and R. Abgrall. Introduction to residual distribution methods. In *34th VKI CFD Lecture Series Very-High Order Discretization Methods*. VKI Lecture Series, 2005.

[8] H. Nishikawa. Divergence formulation of source term. *J. Comput. Phys.*, 231:6393–6400, 2012.

[9] H. Nishikawa and P. L. Roe. On high-order fluctuation-splitting schemes for Navier-Stokes equations. In C. Groth and D. W. Zingg, editors, *Computational Fluid Dynamics 2004*, pages 799–804. Springer-Verlag, 2004.

[10] M. Ricchiuto, N. Villedieu, R. Abgrall, and H. Deconinck. On uniformly high-order accurate residual distribution schemes for advection-diffusion. *J. Comput. Appl. Math.*, 215:547–556, 2008.

[11] R. Abgrall, G. Baurin, A. Krust, D. de Santis, and M. Ricchiuto. Numerical approximation of parabolic problems by residual distribution schemes. *Int. J. Numer. Meth. Fluids.*, 71:1191–1206, 2013.

[12] D. Caraeni and L. Fuchs. Compact third-order multidimensional upwind discretization for steady and unsteady flow simulations. *Comput. Fluids*, 34:419–441, 2005.

[13] G. Rossiello, P. De Palma, G. Pascazio, and M. Napolitano. Third-order-accurate fluctuation-splitting schemes for unsteady hyperbolic problems. *J. Comput. Phys.*, 222:332–352, 2007.

[14] C.-S. Chou and C.-W. Shu. High order residual distribution conservative finite difference WENO schemes for convection-diffusion steady state problems on non-smooth meshes. *J. Comput. Phys.*, 224:992–1020, 2007.

[15] A. Katz and V. Sankaran. An efficient correction method to obtain a formally third-order accurate flow solver for node-centered unstructured grids. *J. Sci.Comput.*, 51:375–393, 2012.

[16] B. B. Pincock and A. Katz. High-order flux correction for viscous flows on arbitrary unstructured grids. In *21st AIAA Computational Fluid Dynamics Conference*, AIAA Paper 2011-2566, San Diego, California, June 2013.

[17] Y.-K. Chen and F. S. Milos. Ablation and thermal response program for spacecraft heatshield analysis. *J. Spacecraft and Rockets*, 36:475–583, 1999.

[18] M. Mahzari, R. D. Braun, T. White, and D. Bose. Preliminary analysis of the mars science laboratorys entry aerothermodynamic environment and thermal protection system performance. In *51st AIAA Aerospace Sciences Meeting including the New Horizons Forum and Aerospace*, AIAA Paper 2013-0185, Grapevine, Texas, January 2013.

[19] D. Bose, T. White, M. Mahzari, and K. Edquist. A reconstruction of aerothermal environment and thermal protection system response of the mars science laboratory entry vehicle. In *American Astronomical Society 221st Meeting*, AAS 2013-311-0712, Long Beach, California, January 2013.

[20] N. R. Merski. Reduction and analysis of phosphor thermography data with the IHEAT software package. In *36th AIAA Aerospace Sciences Meeting and Exhibits*, AIAA Paper 98-0712, Reno, Nevada, January 1998.

[21] T. J. Horvath and s. A. Berry and b. R. Hollis and d. S. Liechty and h. H. Hamilton and n. R. Merski. X- 33 Experimental Aeroheating at Mach 6 Using Phosphor Thermography. *J. Spacecraft and Rockets*, 38:635–645, 2001.

[22] M. Ricchiuto, R. Abgrall, and H. Deconinck. Application of conservative residual distribution schemes to the solution of the shallow water equations on unstructured meshes. *J. Comput. Phys.*, 222:287–331, 2007.

[23] R. Abgrall. Toward the ultimate conservative scheme: following the quest. *J. Comput. Phys.*, 167:277–315, 2001.

[24] W. A. Wood. Equivalence of fluctuation splitting and finite volume for one-dimensional gas dynamics. NASA TM-97-206271, 1997.

**LaTeX Source Files**

**Click here to download LaTeX Source Files: Alireza-Hiro-CAF2014-rev.zip**